Comparison studies in Optimization of Response Variable of Natural Fiber Reinforced Epoxy Composite and Delrin

A Thesis Submitted
In partial fulfillment for the award of the degree of

MASTER OF TECHNOLOGY
IN
PRODUCTION ENGINEERING

SUBMITTED BY
SUSHEEM KANWAR
ROLL NO. - 2K18/PIE/20

UNDER THE GUIDANCE OF

PROF. RANGANATH SINGARI
HEAD, DEPT. OF DESIGN

MR. RAVI BUTOLA,
ASST. PROFESSOR

DEPARTMENT OF MECHANICAL, PRODUCTION & INDUSTRIAL AND AUTOMOBILE ENGINEERING
DELHI TECHNOLOGICAL UNIVERSITY
BAWANA ROAD, DELHI-110042

JULY 2020

CANDIDATE'S DECLARATION

I, SUSHEEM KANWAR, hereby certify that the work which is being presented in this thesis entitled "**Comparison studies in Optimization of Response Variable of Natural Fiber Reinforced Epoxy Composite and Delrin**" being submitted by me is an authentic record of my own work carried out under the supervision of **Dr. Ranganath M. Singari,** Professor, Department of Mechanical Engineering, Delhi Technological University, Delhi and my co-advisor **Mr. Ravi Butola**, Assistant Professor, Department of Mechanical Engineering, Delhi Technological University.

The matter presented in this thesis has not been submitted in any other University/Institute for the award of M.Tech Degree.

SUSHEEM KANWAR

(2K18/PIE/20)

CERTIFICATE

I, SUSHEEM KANWAR, hereby certify that the work which is being presented in this thesis entitled "**Comparison studies in Optimization of Response Variable of Natural Fiber Reinforced Epoxy Composite and Delrin**" in the fulfillment of requirement for the award of degree of Masters of Technology submitted in the Department of Mechanical Engineering at Delhi College Of Engineering, Delhi University, is an authentic record of my own work carried out during a period from August 2019 to July 2020, under the supervision of Dr. Ranganath M. Singari, Professor, Department of Mechanical Engineering, Delhi College of Engineering, Delhi and Mr. Ravi Butola, Assistant Professor, Department of Mechanical Engineering, Delhi Technological University.

The matter presented in this thesis has not been submitted in any other University/Institute for the award of M.Tech Degree.

Dr. Ranganath M. Singari
SUPERVISOR
Professor, Deptt. Of Mechanical Engg.
Delhi Technological University,
Delhi-110042

Mr. Ravi Butola
CO-SUPERVISOR
Asst. Professor, Deptt. Of Mechanical Engg.
Delhi Technological University,
Delhi- 110042

ACKNOWLEDGEMENT

It is my great honour to present my dissertation on "**Comparison studies in Optimization of Response Variable of Natural Fiber Reinforced Epoxy Composite and Delrin**". First and foremost, I am profoundly grateful to my supervisor **Dr. Ranganath M. Singari, Professor, Department of Mechanical Engineering and HOD Department of Design** for his expert guidance and continuous encouragement during all stages of my thesis. I feel privileged on being able to work with him. His analysis and perspective really helped me tackle problems in a novel way. I am thankful to the kindness and generosity shown by him towards me, and for motivating even during the trying times of COVID-19.

I would further like to extend my heartfelt gratitude towards **Mr. Ravi Butola** for helping me accomplish my goals by helping me break down my tasks into small manageable chunks which were to be completed in a time-bound manner. This helped me develop discipline while completing my project.

I would be remiss if I did not appreciate **Dr. Vipin, HOD Department of Mechanical Engineering, DTU** who was always there for me if I needed anything. He was always very approachable and one could come to him with any queries without hesitance. His support has proven to be invaluable to me in the completion of my thesis.

I would further like to thank, **Mr. Shadab Ahmed** (PhD Student) and **Sh. Sunil Kumar** (Machine Shop, CWS) for all their assistance during execution of this project work, without their support it would be almost impossible to complete my thesis work on time.

Last, but not the least, I would like to thank **my family** without whose constant help, encouragement and prayers this would not have been possible.

Date:

Place:

SUSHEEM KANWAR

(2K18/PIE/20)

ABSTRACT

Climate change has necessitated the development of “green” alternatives to replace existing materials. This focus has resulted in the push towards fabricating natural fiber reinforced polymer composites. This research work looks at rice husk ash and groundnut shell ash reinforced epoxy composites as well as the polymer Delrin which are promising alternatives to metal composites for a wide variety of applications. Wear test on the epoxy composites was done using ball on flat tribometer under room temperature. A 6mm steel ball was used as a counter body and 4 different epoxy composite samples of 3cmx3cm were used as the flat. The 4 samples were: neat epoxy, epoxy reinforced with rice husk ash, epoxy which was reinforced using ash of groundnut shell and epoxy reinforced with both ash of rice husk as well as ash of groundnut shell. Upon carrying out the wear test it was found that neat epoxy composite had the maximum wear rate of 163 mm^3/Nm, whereas epoxy composite reinforced with both rice husk ash and groundnut shell ash was the most resistant to wear. Apart from wear test, the surface roughness of all the nine composite samples was measured and optimization through the implementation of genetic algorithm (GA) was done. It was found that a minimum surface roughness of 1.503μm can be obtained for an epoxy-hardener ratio of 2.99:1 and without the addition of any reinforcements. This optimization was achieved within 102 generations. Apart from GA, response surface methodology (RSM) and Taguchi design of experiments was carried out as well to optimize and the results obtained closely agreed with those obtained from GA. RSM gave an optimized surface roughness value of 1.39μm and the main effects plot showed that the best combination of input factor was a 3:1 ratio of epoxy to hardener with 0% reinforcement. Analysis of Variance (ANOVA) showed epoxy to hardener ratio as the most significant factor contributing 36.35% of the total effect. Similar to the epoxy composites, optimization of response variables through GA, RSM and Taguchi design of experiments was carried out for Delrin as well and the results compared. GA gave an optimized value of 0.351μm surface roughness and 1788.91mm^3/min material removal rate within 139 generations for a speed of 150rpm, feed of 0.6mm/rev and 1.49mm depth of cut. On the other hand, RSM gave an optimized value of 0.736μm surface roughness and 2436mm^3/min material removal rate for a speed of 192.42rpm, 0.458 mm/rev feed and 1.5mm depth of cut and Taguchi gave the best combination of input values as 150rpm speed, 0.6 mm/rev feed and 1.5mm depth of cut. These values closely agreed with that of GA. ANOVA showed depth of cut was the most significant factor contributing 57.72% of the total effect.

Keywords: Natural Fiber, Composite , Genetic Algorithm, Response Surface Methodology, Taguchi, Analysis of Variance

CONTENTS

LIST OF FIGURES

Chapter 1: INTRODUCTION

Chapter 3: EXPERIMENTAL SET UP

Chapter 4: RESULTS AND ANALYS

LIST OF TABLES

Nomenclature

Abbreviations	Full-Form
Ra	Arithmetic average of roughness
SR	Surface Roughness
DOE	Design of Experiment
GA	Genetic Algorithm
RHA	Rice Husk Ash
GSA	Groundnut Shell Ash
RSM	Response Surface Methodology

CHAPTER 1

INTRODUCTION

This paper focuses on natural fiber reinforced composites. Using natural fibers as reinforcements is beneficial to the environment and therefore a lot of emerging research deals with using natural fibers as reinforcements in composites.

1.1 Natural Fibers

They led to a switch in focus from merely fabrication of composites to fabrication of composites which were reinforced with natural fibers. Use of these fibers as reinforcement material serves a dual purpose: (a) It helps us recycle waste material like jute straw, bamboo stalk, rice husk, groundnut shell etc.[1] which would otherwise have been disposed off. (b) Natural fiber is biodegradable and eliminates the use of energy intensive synthetic fibers, thus, it is more eco-friendly [2]. In addition to being more environmentally friendly, natural fibers possess the added advantage of being easily available, non-toxic, having higher specific strength, light weight, low cost and more resistant to abrasion.[3-10].

For all their advantages, natural fibers aren't a miracle cure and have limitation of their own. Their hydrophilic nature leads to them absorbing great quantities of moisture [11] which results in bonding between matrix and reinforcement which is weak at the interface [12]. This greatly affects the composite attributes [13-14]. Though chemically treating natural fibers with 5-6% NaOH improves interfacial bonding, it also increases the surface roughness of the component[15].

1.1.1 Rice Husk Ash (RHA)

One of the natural reinforcements utilized for this research is Rice Husk Ash (RHA). One reason it has been selected is because this crop is grown in huge numbers throughout the planet, with the husk of the rice accounting for about 130 million tons of agricultural waste produced globally every year [16-17]. Moreover, rice husk (the waste product obtained upon burning rice paddy) has no commercial use, therefore, in many developing countries it is simply burnt away leading to pollution [18]. This fact led to research focusing on the utilization of rice husk to prevent waste. Over the last few decades some headway has been made regarding the use of RHA in light weight construction material [19-20]. There is an economic incentive to extract silica from rice husk as silica is about 80-90% by weight of the rice husk [21]. This is good news, especially for rice producing nations like India,

Vietnam, Thailand, etc. There are several advantages of extracting silica from rice husk. Silica can be treated to form SiO_2 which has several applications in industry [22-29]. Kapur et al [30] performed pin-on-disk abrasive wear test on neat PVC sample and RHA reinforced composites. They found that rice husk composites displayed lower wear or damage. A BOD machine was used to perform abrasive wear tests on RH reinforced composites in wet and dry conditions between loads of 0.98-9.8N and velocities of upto 1 m/s . Research has shown that both friction as well as rate of wear, are higher when subjected to wet conditions due to the formation of a hydrophilic silica-rich layer in dry conditions which mitigated the effects regarding friction between conjoined surfaces [31].

1.1.2 Groundnut Shell Ash (GSA)

The other reinforcement utilized for this research paper is groundnut shell ash. China and India are the two biggest producers of groundnut in the world. India alone produces around 7.5 million tons of groundnut [32]. Thus, disposal of groundnut is of grave concern. Using groundnut as reinforcement in composites helps in eliminating waste. Groundnut ash powder of size upto 1 micro-metre was utilized for reinforcing composites like polypropylene [33]. It was found that there was a considerable increase in mechanical attributes like impact, flexural and tensile strength, along with modulus of composites. A positive correlation was found between the increase in these properties and the reinforcement percentage and powder size and an inverse relation with the strain generated in the composite. Usman et al. compared polyethylene composites reinforced with alkaline treated groundnut shell powder and non-alkaline treated groundnut shell powder. It was observed that alkaline-treated groundnut powder reinforced composites showed a higher increase in mechanical attributes alongside biodegradability and lower rate when it comes to absorption of water [34]. Groundnut shell was determined to have moisture content in the range of 1.92-4.96% [35]. Brian George et al. characterized groundnut shell reinforcement fibers and found the fiber to have a length of about 38mm with a diameter of about 0.25mm [36].

1.1.3 Chemical composition

Fibers obtained from natural sources are mainly composed of hemicellulose, cellulose(main component of the fiber) and lignin (binds the fiber together). Table 1.1 shows the chemical makeup of groundnut shell as well as rice husk.

Table 1.1: Chemical Composition of groundnut shell and rice husk.

	Cellulose (wt%)	Hemicellulose (wt%)	Lignin (wt%)	References
Rice Husk	31.3	24.3	14.3	[37]
Shell of Groundnut	35.7	18.7	30.2	[38]

For obtaining best properties from the materials, we make use of composites as they have been in existence since time immemorial. Early humans used bricks made out of mud coupled with easily available substances like straw [39]. These were a rudimentary form of composites. Composites are basically a mixture of multiple entities, with the final concoction possessing properties of its constituent elements. This allows composites to have the "best of both worlds". One component is known as the matrix, while the other is the reinforcement. The reinforcement is responsible for bearing the load the composite is subjected to [40-41]. Initially, metal composites were overwhelming used, however, the discovery of polymers has revolutionized the world of composites with the introduction of synthetically reinforced composites which possessed much of the properties of metal composites while being cheaper alternatives [42-44]. Polymer materials can be of 2 types, thermosetting and thermoplastic. One thermoplastic polymer which has shown a lot of promise is Delrin. Delrin is a thermoplastic polymer trademarked by DuPont and commonly known as polyoxymethylene (POM). It is produced by the polymerization of formaldehyde and has gained widespread recognition all over the world for reliability of performance in thousands of engineering components. After its introduction in 1960, it has been used in various fields of automotive, appliance, construction, hardware, and electronics industries consumer goods. Delrin® is the DuPont registered trademark for its brand of acetal resin also commonly referred to as polyoxymethylene (POM). Glass fiber reinforced plastic was found to have maximum impact strength in wet layup process[45]. They thus proved to be effective replacements, especially for non-high load bearing applications. This advantage of the polymer composite has led to a proliferation in its use in a myriad industries ranging from automotive and aerospace to biomedical. However, there is a growing need to shift to more "green" or eco-friendly production of composites [46].

According to a report released by UN Intergovernmental Panel on Climate Change (IPCC) humanity has a limited time period of 12 years to keep the average temperature rise below 2 degrees celcius [47](the threshold beyond which we'll lose ice cover in the Artic during summers leading to widespread catastrophe). Currently there are some difficulties associated

with shifting to more “green” alternatives, since many of the composite have crude oil as their raw material. Oil extraction and transport leads to severe environmental problems in the form of oil spills, which in turn lead to destruction of the flora and fauna of that region in addition to displacing the inhabitants of those lands [48]. Furthermore, producing polymers and synthetic reinforcements from crude oil is an extremely energy intensive process. Thus a lot of fossil fuels are currently burned to fabricate the polymers and fibers currently employed in industry [49-50].

Lathe machine is the most utilized machine in manufacturing used to fabricate cylindrical components. They cut work pieces while they are rotated. A variation on the conventional lathe machine, known as the CNC lathe is capable of producing precision cuts and increase productivity. They are mostly intended to manufacture components which would be infeasible to make conventionally.

CNC lathes and CNC milling machines can be programmed via G-code and M-code. CNC’s are extremely versatile allowing you to produce a myriad of products and materials. This varies with size, flexibility and power of the machine. CNC machines have been known to cut wood, plastics, metals and composites and offer benefits like greater flexibility and productivity, as well as improved reliability, quality, and scrap rate. A whole host of different industries like aerospace, electronics, automotive sectors, firearm manufacturing, etc. make use of them, especially where quality of surface is paramount. Good surface properties result in increased fatigue strength and creep life, as well as resistance to corrosion. In addition to this, SR affects, numerous functional qualities of components, for example wear, heat transmission, facility of holding lubricant, coating as well as fatigue resistance. It is also instrumental with regards to controlling and assessing the surface quality of a product.

One of the most widely utilized models for figuring out the SR is where surface roughness (R_a) is determined using feed rate (f) as well as nose radius (r) via the relation $f^2/32r$. From the previous equation it can be observed that factors which influence SR the most are f and r [51-52]. Decrease of SR quality is directly proportional to decreasing product value. In field of production, particularly in engineering, the surface finish quality can be a significant importance that can affects the working of a component, and possibly its cost, especially in critical situations like engineering components subjected to fatigue loads, et cetera.

SR is one of the greatest vital constraints in the field of machining and manufacturing. And thus cutting parameters selection is so important in any machining process. Manufacturing industries focus a lot of their resources on their product quality. They aim to manufacture components of exceptional quality within a specified length of time in a cost effective manner. Surface finish obtained, is an extremely critical performance parameter that has to be constrained within the margin of error for the process under consideration. Due to its importance, investigation of SR with a view to better understand and control it has been a growing. It has been observed that there are several parameters which can be easily controlled like feed, speed, depth of cut etc., while factors such as tool wear, machine vibration, material defects etc. display a lot more variability and are not easy to control. Usually we try to obtain surface roughness below the threshold for our application by controlling the values of input parameters. SR is also responsible for numerous functional characteristics of components, for example contact which generates friction on the surface, wear, reflection, transmission of heat, ability to hold and dispense a lubricant, coating or opposing fatigue. As a result, the preferred value of the finish to be obtained on the surface is clearly stated beforehand and the factors selected in such a manner as to obtain the requisite value. Novel research in the area of monitoring of tool condition shows people are aiming to acquire a robust as well as an exact model that is capable of finding a relationship between cutting parameters as well as SR of the machined products.

1.2 Types of Roughness

Roughness generated on the machined surface is classified as comprising of 2 autonomous effects: Ideal and Natural roughness.

1.2.1 Ideal Roughness

Ideally roughness found to be dependent on only feed and geometry. Under such a condition the finest finish that is possible for a specified shape of tool and feed is obtained. This is possible when limitations like built-up-edge (BUE), chatter as well as inaccurate movements of the tool are rendered moot. In order to determine greatest unevenness height for a tool which is sharp and sans nose radius, we use the equation given below:

$$\mathbf{R\ max = f / (\cot \varphi + \cot \beta)}$$

The SR value given by:

$$\mathbf{Ra = Rmax / 4}$$

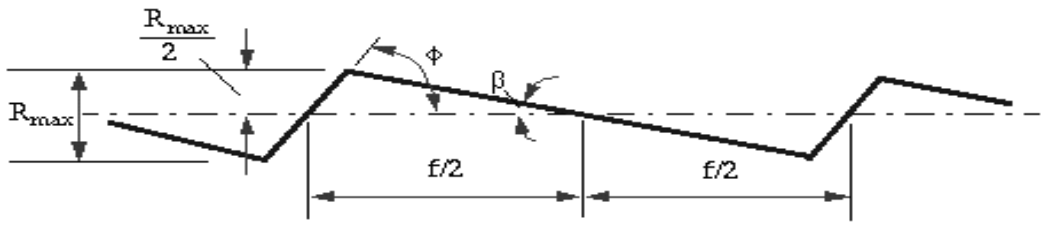

Figure 1.1 Surface profile

Here 'f' refers to feed, Φ refers to the major cutting angle and β is the minor cutting angle.

1.2.2 Natural Roughness

Built-up edge has a significant contribution in the creation of natural surface roughness. Thus, greater the built up edge, greater the roughness on the surface. Factors which reduce friction at chip-tool interface and eradicate built-up edge tend to generate superior surface finish. Profile of tool can be varied to achieve a better finish [53].

1.3 Taguchi Method

Taguchi's parametric design is a robust design which was used as an easy and organized qualitative alternative at a relatively low cost[54-55]. Taguchi method as used in the area of QC involves every step in the product life cycle. Albeit, the most crucial criteria for attaining high quality at low cost is dependent on DOE which determines the result when cutting variables such as speed, feed, and DOC are varied, with the objective of obtaining a value of SR which is suitable for mild steel for a given application, while the mild steel job had been machined with a carbide tool [56]. Taguchi method can evaluate signal-to-noise ratio in 3 different ways:

(a) **Smaller-the-Better**: n = -10 Log_{10} (avg. sum of squares of experimental results).

The user selects this option when SN ratio evaluated for properties which are typically undesirable and whose ideal value is zero, for example " defects " etc.

(b) **Larger-the-Better**: n = -10 Log_{10} (avg. sum of squares of the reciprocal of the results)

(c) **Nominal-the-Better**: n = 10 Log_{10} (square of mean/ variance).

Used when property selected is the most wanted, that is, highest possible value is preferred.

1.3.1 System Design

Here the engineering know-how of an engineer is used for generating a prototype, which includes both the product as well as the process design. When it comes to the product design stage, materials, parts, uncertain product variable values, etc., can be chosen. On the other hand the process design stage consists of evaluation of sequences used in processing, choosing of equipment for production, provisional values of process variables, etc. due to the fact that system design is an initial functional design, which oft deviates from optimal values of quality and cost. System design, is extremely creative and innovative.

1.3.2 Parameter Design

Parameter design enhances results of refining features as well as helps in identifying parameter values. Moreover, ideal values of the process variable attained from the parameter design do not change with change in environmental factors. As a result, this design is significant in accomplishing great quality without any cost increase. Therefore, more experiments need to be carried out by increasing values of the process variables and we achieve this using orthogonal arrays, in order to examine the whole design using limited amount of experiments. A loss function expresses discrepancy between experimental and desired value. Taguchi utilizes a loss function for computing performance characteristic. It is then altered to signal-to-noise (S/N) ratio; typically 3 characteristics exist in S/N ratio, namely, nominal- the-better, higher-the-better, and lower-the-better [57].

1.3.3 Tolerance Design

By understanding the consequence the myriad variables on performance, tolerance design can be utilized for focusing resources in reducing as well as regulating deviation in the critical dimensions.

1.4 Design of Experiments (DOE)

It is a technique for modeling as well as analyzing the influence of process parameters over an output [58]. DOE is the most widespread technique for product or process developments. It aims to predict a multi-parameter process in just a few trials via statistics.

1.5 Full Factorial Design

In this the experimental data comprises of all possible combinations depending on the input factors. Such a DOE allows us to determine the significance of every factor on output, and effects of connections among factors and response variable. If the design consists of k factors with 2 levels each; 2^k runs are observed. Steps of Taguchi method are as follows [59-60]:

(a) Figuring out the main function, side effects and identifying the failure mode.
(b) Figuring out noise factor along with quality traits and testing conditions.
(c) Figuring out function which needs to be optimized.
(d) Determining the factor which is governing along with its levels.
(e) Choosing OA and matrix.
(f) Carrying out the matrix experiment.
(g) Analyzing and forecasting based on data obtained to optimize performance.
(h) Verification results of the experiment and making plans for the future.

1.6 ANOVA

Due to the vast quantity of variables monitoring the end result, some kind of generalization is required which is achieved using mathematical models. Since these models are our best approximation based on our understanding of the given phenomena, they mostly comprise of just the most influential parameters. One of the major and widely used statistical tools is analysis of variance or ANOVA. It helps user by determining the relative contribution towards the final outcome.

ANOVA gives us the percentage that an input parameter influences the response variable/s and thus is a useful tool to interpret experimental data. Ratio of variances determines implication of the experiment statistically. This ratio has proven to be independent of modifications to the experimental dataset in addition to being independent of constant bias as well as scaling errors.

CHAPTER 2

LITERATURE REVIEW

2.1 Tribology: Wear and Coefficient of friction (COF)

Despite the best efforts of maintenance engineers, there are bound to be economic losses [61], increasing time consumption in operation [62] and inefficiency in operation [63] due to wear and tear experienced by mating systems during the life cycle of the components leading to eventual failure [64]. Thus, there is a need to develop novel material systems to increase durability and efficiency of the tribo-system. Over the past few decades, many researchers introduced polymer composites as a solution to this problem [65-66]. Recently, the U.N. World Commission on Environment and Development has issued a call to action to minimize and replace the synthetic reinforcements in polymer composites with natural fibers [67]. This is part of its push towards "green tribology" which involves conservation of energy as well as promotion of eco-friendly alternatives to current materials. This increased focus on natural fiber reinforcement for tribo-composite applications has led to the current century being dubbed the "cellulosic century" [68]. Many components like bearings, break shoes, shafts etc. undergo failure due to friction and wear experienced during operation and thus need to be assessed for tribological behavior [69]. Before a material is allowed to be used in practice it is subjected to friction and wear tests to gauge its performance [70-71]. Wear is of various types. Abrasive wear occurs due to sliding action between mating surfaces under pressure [72] while fatigue wear happens gradually at the end of a particular number of cycles. The load subjected onto the component with each cycle leads to surface and sub-surface cracks along with the generation of debris. Type of wear generated is highly correlated with the type of matrix used.

The equations governing the tribological properties are given below [73-74]. These properties are primarily a measure of friction coefficient (COF) as well as specific wear rate.

For specific wear rate: $k = \Delta m/\rho L F_n$ or $k = 2a\Delta h/nIA\omega^2$

For friction coefficient: $\mu = F/R$

k = specific rate of wear (m^3/J), Δm = loss in mass (g), L = travel length (m), F_n = normal load (N), a = area of contact (m^2), I = moment of inertia (kgm^2), ω = angular speed (rad/s), Δh = reduction in thickness (m)

A study conducted on polyamide and polyphenylene based composites at a 15N load along with a 1000 r/min speed showed that increase in load is directly proportional to both wear

rate as well as friction coefficient but an inversely proportional relationship exists between speed and friction coefficient and a direct relationship exists between speed and wear rate [75]. Addition of carbon nanotubes as reinforcement in polymer composite led to a deterioration in tribological properties of the component [76]. Carbonization temperature was found to significantly affect both wear and friction. A study which investigated this phenomena, found that for rice husk ash based composites, a carbonization temperature of 950 degrees celsius was optimum for decreasing the composite wear rate [77]. Imrek et al. discovered pressure was directly proportional to wear uptil a maxima of 5 MPa, after which the wear rate decreased as a result of transfer film formation at the interface [78].

A lot of research has looked at result of DOC, feed, and nose radius, speed etc. on SR, which greatly influences wear of a material. A few of these papers have been briefly explained below.

Ranganath M.S. et al. [79], examines effect of variables upon turning on SR of Aluminium 6061. Input factors were speed, feed and DOC. DOE was carried out for figuring out influence of input factors on SR. ANOVA and F-test showed the most influential variable is feed, with DOC and speed following it. Optimal values for various input variables are shown to be 2100 rpm, 0.1 mm/rev and 0.2mm. This combination gives the least surface roughness. Regression is used for determining surface roughness which makes fairly accurate predictions within a margin of error.

Ilhan Asilturk et al. [80] optimizes turning parameters in order to achieve the least SR. L9 orthogonal array (OA) has been utilized to run trials of CNC turning. Job was a AISI 4140 (51 HRC) and cutting tools were carbide coated. Every experiment was done thrice in order to get accurate readings. ANOVA was used in examining effects of input parameters on response variable, i.e. SR. Feed rate proved to have the greatest influence on Ra and Rz. Optimal values of cutting variables, corresponding to least SR in turning were 120 m/min for speed, 0.18 mm/rev feed and 0.4 mm DOC.

Davim.J et al. [81] did their research on SR predictive models through ANN for figuring out the influence of cutting variables on 9SMnPb28k(DIN). Artificial neural network (ANN) technique used in determining SR parameters (Ra and Rt) consists of feed, speed and DOC as inputs. L27 orthogonal array formed the basis of the experiments with each factors

possessing 3 levels. ANN helps examine interaction between cutting parameters and response variables thorough 3D surface plots. The analysis found that speed and feed are majorly responsible in minimizing surface roughness, while DOC does not have as much influence over the response variable as the other 2 parameters. When DOC is low, SR is extremely sensitive to cutting speed; and an inverse relationship exists between them. However, this decrease in SR keeps on reducing, more the DOC is increased. Research has shown that SR variation is negligible with change in DOC at higher values of cutting speed. Surface roughness has proven to directly proportional to feed rate.

I.A. Choudhury et al. [82] developed models for predicting SR during turning of EN 24T steel (290 BHN) via RSM. Primary cutting variables like speed, DOC, feed have been examined using a factorial design and uncoated carbide inserts without any cutting fluid. Speed in the region of 36-117 m min^{-1} and 28-150 m min^{-1} has been depicted. Moreover, it has been found that RSM along with factorial DOE is better in comparison to conventional one- variable-at-a-time methods used to investigate influence of input parameters on output variables like SR and life of tool. This technique offers the benefit of decreasing number of experiments, making the entire experimentation process economically feasible. Feed is shown to possess a more significant influence in contrast to cutting speed and DOC.

W.H. Yang et al. [83] uses Taguchi technique, for determining best combination of values of cutting variables in turning. An OA, and ANOVA were utilized for determining S45C steel bars characteristics by utilizing cutting tools made of WC. Confirmation experiments were carried out to cross-check these values. Tool life and SR were found to improve by about 250%.

M. Nalbant et al. [84] tried to find optimum values of input variables in turning process involving AISI 1030 steel bars with tools coated using TiN. 3 input variables were used: insert radius, feed rate, as well as DOC. Insert radius and feed determined as the most influential variables influencing surface roughness. It was found that by using higher insert radius (1.2 mm), lower feed (0.15 mm/rev) as well as lower DOC (0.5 mm) a much superior SR was obtained. Change in SR between initial and optimal cutting values is around 335%.

2.2 Linear Regression

An equation gives the linear relationship between independent and dependent variables [85]. Most widely used regression technique due to its simplistic nature where the dataset changes linearly and therefore is easier to fit compared to other non-linear datasets[86-87]. For *n* points present in a dataset, linear regression models assumes a linear correlation between x and y. There will be some error/noise in each model which gets included as depicted below:

$yi = \beta 01 + \beta 1x1 + \ldots. \beta nxn + \varepsilon i = \mathbf{x}^T \boldsymbol{\beta} + \varepsilon i$ where i=1,…n

2.3 KNN Regression

It is among the simplest algorithmic techniques in machine learning. The average of K nearest values is considered to be the value of interest or the desired value. KNN regression technique is a non- parametric type of regression analysis [88].

2.4 Support Vector Regression (SVR)

SVRs are a type of supervised learning model that give continuous output for a given input. They come under the category of support vector machine (SVM) or support vector network [89]. The objective of SVR regression is to determine a function that maximizes deviations for all the data points[90]. Values should be less than the threshold of ε to be neglected, otherwise they are considered to be unacceptable [91]. Linear support vector regression has a general equation:

$y = \Sigma i=1(ai - a)\langle xi,x\rangle + b$

2.5 Bayesian Ridge Regression

Bayesian regression prevents overfitting by making use of a regularization parameter. Bayesian ridge regression estimates β using L2-constrained least squares [92]. Scaling is hard due to the sheer number of samples present, but the weights are shifted toward zeros, which results in stability. The implementation studied is taken from [93] and better regularization parameters values determined from the ones mentioned in [94].

2.6 Decision Tree Regression

It involves dividing dataset into smaller subsets represented by leaf nodes [95]. Node corresponding to best predictor is referred to as the root node.

2.7 Gradient Boosting Regression

It is an ensemble ML model. The various ML models are generalized by allowing optimizing on an appropriate cost function [96]. Gradient Boosting model helps in optimizing loss functions. Function to be minimized is:

$L(y, F(x))$: $F = \text{argmin}_{Ex,y}[L(y, F(x))]$.

2.8 Neural Networks (NN)

Simulate the neuronal architecture of the brain. Consist of a minimum of 3 layers which are referred to as the input, output and hidden layer. Weights are assigned to the coneeections which can take positive, negative or zero value [97]. More the quantity of iterations, better the NN learns. Once it has figured out the relationship, it can generalize unseen data and predict outputs for new input data.

2.9 Genetic Algorithm (GA)

GA is an optimization method where an initial population is randomly generated and the fittest entities from that population are chosen to pass on their “genes” to the next generation. This step is known as selection. By mating the selected entities new “Offspring” can be generated. GA algorithm goes through a number of iterations till the offspring produced are not much different from the parents. This point is known as convergence [98-100].

The objective of this thesis is to:

1. Use regression techniques to predict the value of response variables in machining of Delrin.

2. Optimize the response variables for Delrin using GA, RSM and Taguchi DOE and compare the results.

3. Find the statistically most significant input factor in machining of Delrin using analysis of variance (ANOVA).

4. Fabricate RHA and GSA reinforced epoxy composites.

5. Use regression techniques to predict the value of response variables for epoxy composite samples.

6. Optimize the response variable for epoxy composites using GA, RSM and Taguchi DOE and compare the results.

7. Find the statistically most significant input factor for the epoxy composites using analysis of variance (ANOVA).

8. Determine the wear rate of composites fabricated.

CHAPTER 3

EXPERIMENT SET UP

3.1 Device for determining Surface Roughness

Figure 3.1 shows Surtronic 3+, which is used for determination of surface texture. A microprocessor is used for evaluating all the parameters and other functions and these values are shown on an LCD display as shown in figure 3.2.

Figure 3.1 Surtronic 3+ surface roughness measuring instrument

The device also utilizes a drive motor to move stylus along the surface for measuring surface roughness as shown in figure 3.3. Once the measurement is complete, the stylus returns to the original position. Selection of cut-off (Lc) length used in figuring out the value of length moved by the stylus.

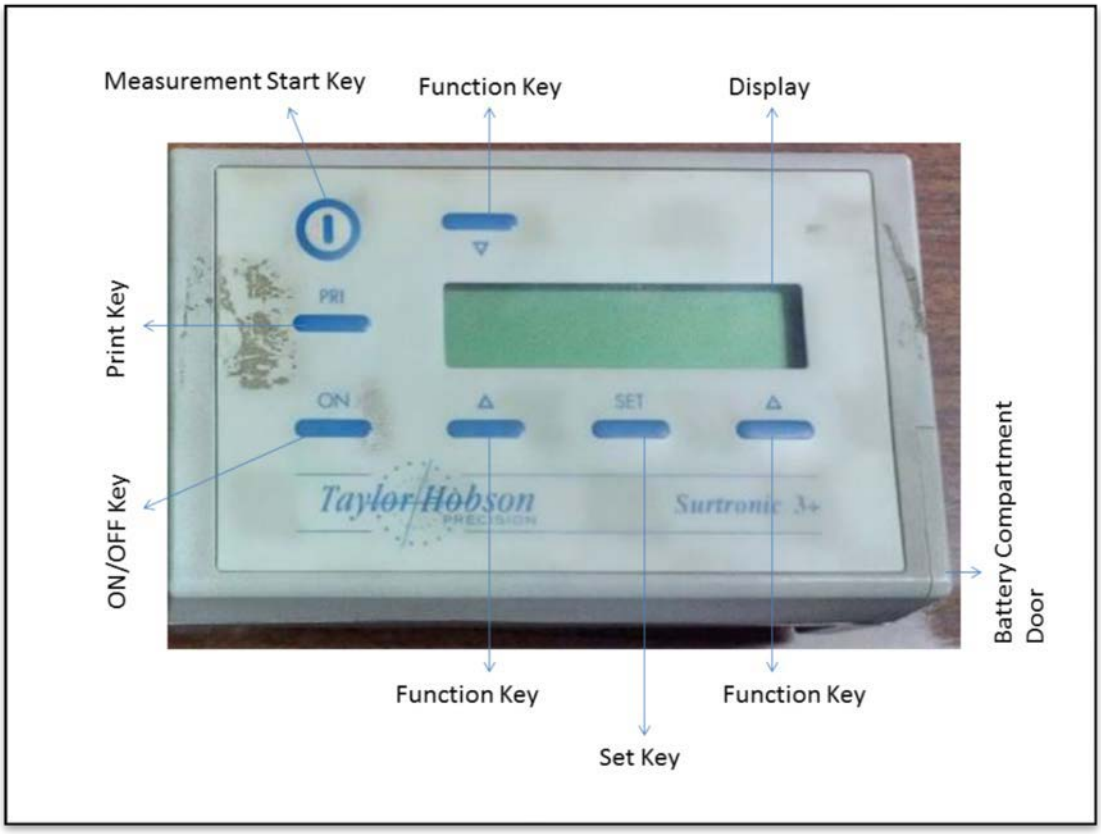

Figure 3.2 Display Transverse Unit (Referred from Instrument Manual)

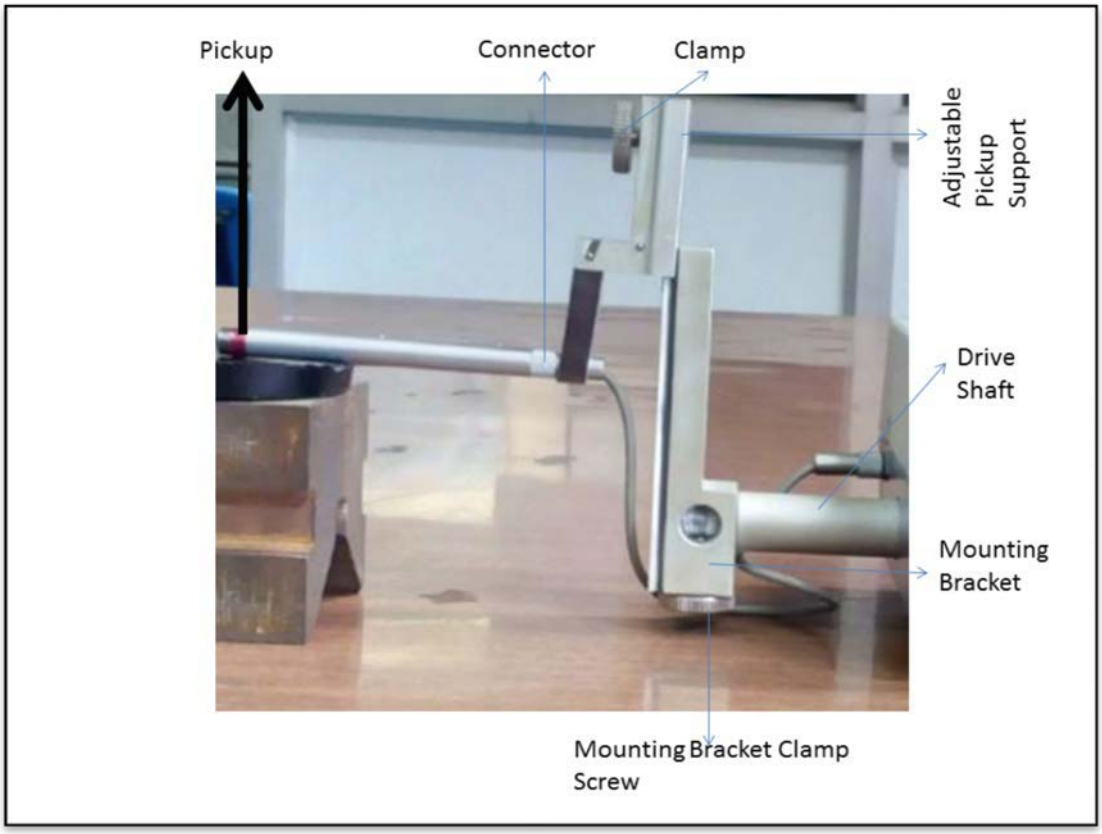

Figure 3.3 Mounting Bracket (Referred from Instrument Manual)

3.1.1 Pick-up

Pick-up forms a variable reluctance style transducer. Figure 3.4 shows the pick-up as it traverses the surface, stylus moves in relation to the skid and these movements change into a corresponding electrical signal. This enables the pick-up to move along the surface without being influenced by roughness, and gives a reference for displaying general profile of the surface.

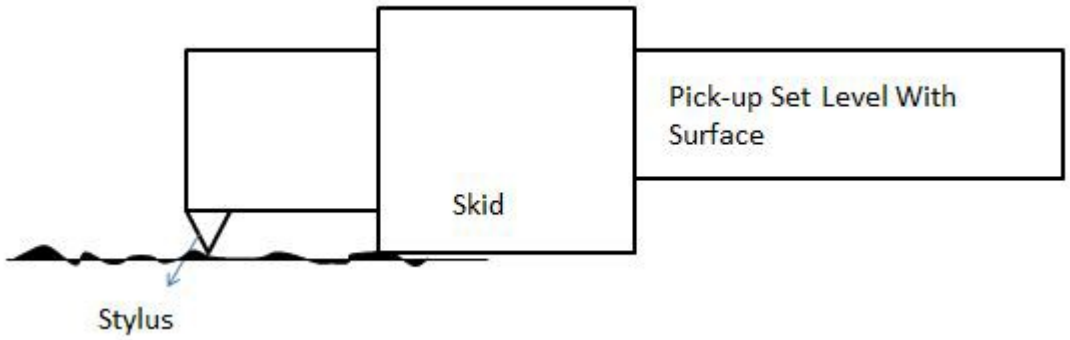

Figure 3.4 Pick-up (Referred from Instrument Manual)

3.2 Measurement of Surface Roughness

SR of the jobs is measured using various measurement strategies which are classified as:

- Direct measuring techniques
- Methods based on comparison
- Non-contact techniques

3.2.1 Direct Measuring Techniques

A stylus is utilized to assess the finish obtained on the surface by moving it over the surface whose SR is to be determined. The movement of the probe perpendicular to the desired surface is considered. The profile obtained is subsequently utilized for determining roughness parameters as shown in figure 3.5. The parameter Ra is used here.

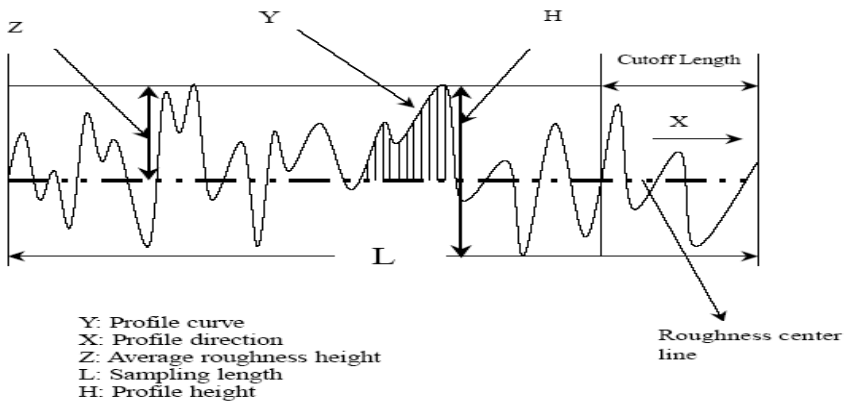

Figure 3.5 Measurement of SR by Stylus [101-102]

3.2.2 Methods based on Comparison

These methods use components fabricated via the same process using the same materials as well as machining variables as the comparison surface. This method used when SR Ra>1.6 micrometers.

3.2.3 Non-Contact Techniques

A luminescent rough surface is achieved via a monochromatic plane wave which is normal to the surface. A sensor is placed at the len's focus and uses a camera for pattern recording. Using this, SR value can be calculated.

3.3 Experimental Procedure

3.3.1 CNC Turning of Delrin

In our paper accepted in the Scopus indexed LNME and presented at the ICAPIE 2019 conference we took 3 different cutting parameters, namely feed (mm/rev), depth of cut (mm) as well as speed (RPM), vary and the corresponding MRR (mm3/min) and surface roughness (micrometres) are represented by a Taguchi L27 orthogonal array. The train_test_split function of sklearn splits the dataset further into two categories: training and testing. Testing data is represents one-third of the entire dataset, with the rest being training data.

A homopolymer Delrin rod of diameter 34 mm was selected and CNC Turning operation was performed on it as shown in figure 3.6. Before performing final CNC Turning operation, a roughing operation was performed on it. At the end the turning operation the diameter was reduced from 34mm to 33mm. In the CNC turning operation three different depth of cuts were provided: 0.5mm, 1.0mm and 1.5mm. The entire rod was broken into three pieces of equal length and all the operations for a particular depth of cut were performed on each rod in succession. Various regression techniques were then applied on the dataset and the mean square error was calculated to determine the accuracy of the ML regression models. The scikit learn library of python was used for implementing the various regression techniques. In addition to regression techniques, a neural network has also been implemented to predict the MRR and surface roughness using the keras library. Matplotlib library has been utilized to plot the experimental MRR and SR values along with the predicted MRR and SR values. MATLAB optimization toolbox is used to implement multi objective genetic algorithm to find the optimized values of the input variables.

Figure 3.6 Turning operation performed on Delrin rod with different input values

CNC Turning experimental data obtained was arranged in a L27 orthogonal array as depicted in Table 3.1:

Table 3.1 L27 ORTHOGONAL ARRAY

Exp No.	Control Factors			Speed (s)	Feed (f)	Depth of Cut (d)	Surface Roughness (Ra)	MRR
	A	B	C	(rpm)	(mm/rev)	(mm)	(μm)	(mm^3/min)
1	1	1	1	150	0.2	0.5	1.04	1083.77
2	1	1	2	150	0.2	1.0	2.44	1784.15
3	1	1	3	150	0.2	1.5	0.56	1120.99
4	1	2	1	150	0.4	0.5	0.90	1665.85
5	1	2	2	150	0.4	1.0	1.42	1568.58
6	1	2	3	150	0.4	1.5	0.96	1898.23
7	1	3	1	150	0.6	0.5	0.86	1702.32
8	1	3	2	150	0.6	1.0	1.14	2505.56
9	1	3	3	150	0.6	1.5	1.16	1933.68
10	2	1	1	250	0.2	0.5	2.62	2140.88
11	2	1	2	250	0.2	1.0	5.38	2216.46
12	2	1	3	250	0.2	1.5	0.52	2538.14
13	2	2	1	250	0.4	0.5	2.32	1811.81
14	2	2	2	250	0.4	1.0	3.58	2469.70
15	2	2	3	250	0.4	1.5	0.64	2040.10
16	2	3	1	250	0.6	0.5	1.92	1410.84

17	2	3	2	250	0.6	1.0	3.44	1532.72
18	2	3	3	250	0.6	1.5	0.94	1579.62
19	3	1	1	300	0.2	0.5	2.04	1047.48
20	3	1	2	300	0.2	1.0	4.80	960.00
21	3	1	3	300	0.2	1.5	1.00	1085.79
22	3	2	1	300	0.4	0.5	2.24	251.998
23	3	2	2	300	0.4	1.0	3.84	461.219
24	3	2	3	300	0.4	1.5	0.80	980.251
25	3	3	1	300	0.6	0.5	2.70	143.928
26	3	3	2	300	0.6	1.0	3.76	0.0035
27	3	3	3	300	0.6	1.5	0.74	0.1408

3.3.2 Epoxy

Matrix for our paper is epoxy resin as shown in figure 3.7. Epoxy resin has myriad advantages like excellent dimensional and thermal stability as well as low moisture absorption. It also displays good mechanical properties because of its low shrinkage structures [103].

Figure 3.7 (From Left to Right) Resins and Hardeners of ratios 2:1, 5:3, and 3:1.

This paper looks at the tribological properties of rice husk ash and groundnut shell ash reinforced epoxy composites. Investigation into polymer composites which have been improved through various additives, is the need of the hour. This paper aims to compare the tribological

characterictics of epoxy composite reinforced with both RHA and GSA with epoxy composites reinforced with either RHA or GSA.

3.3.3 Preparation of RHA and GSA powder

Rice husk and groundnut shell were taken separately and burned and the ash obtained was put inside a ball mill where it was ground for a few hours at an rpm of 600rpm. After milling the powder was successively passed through a series of sieves. The maximum powder was collected at sieve with ASTM no. 200 in both cases. Figure 3.8 shows RHA before processing and after processing to be used as the reinforcement. Figure 3.9 shows GSA before processing and after processing to be used as the reinforcement.

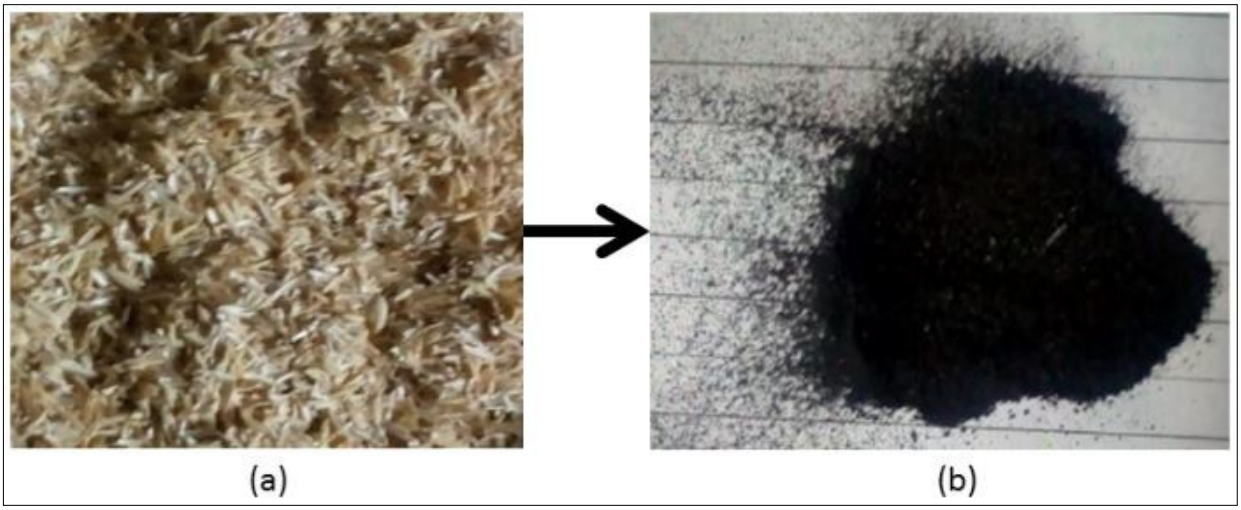

Figure 3.8 (a) Rice husk before burning and ball milling (b) Rice husk ash (RHA) used to make reinforcement for the composite.

Figure 3.9 (a) Groundnut Shell before ball milling (b) Groundnut Shell Ash (GSA) used as reinforcement in epoxy composite

3.3.4 Preparation of composite

Epoxy and hardener were mixed in a 2:1 ratio. In addition to that GSA and RHA powders were added in the required amount after weighing in a digital weight balance. The mixture was then stirred for about 3 minutes and left for 24 hours. Nine different composites were prepared with different combinations of epoxy to hardener ratios and weight percentages of the reinforcements RHA and GSA as depicted in figure 3.10.

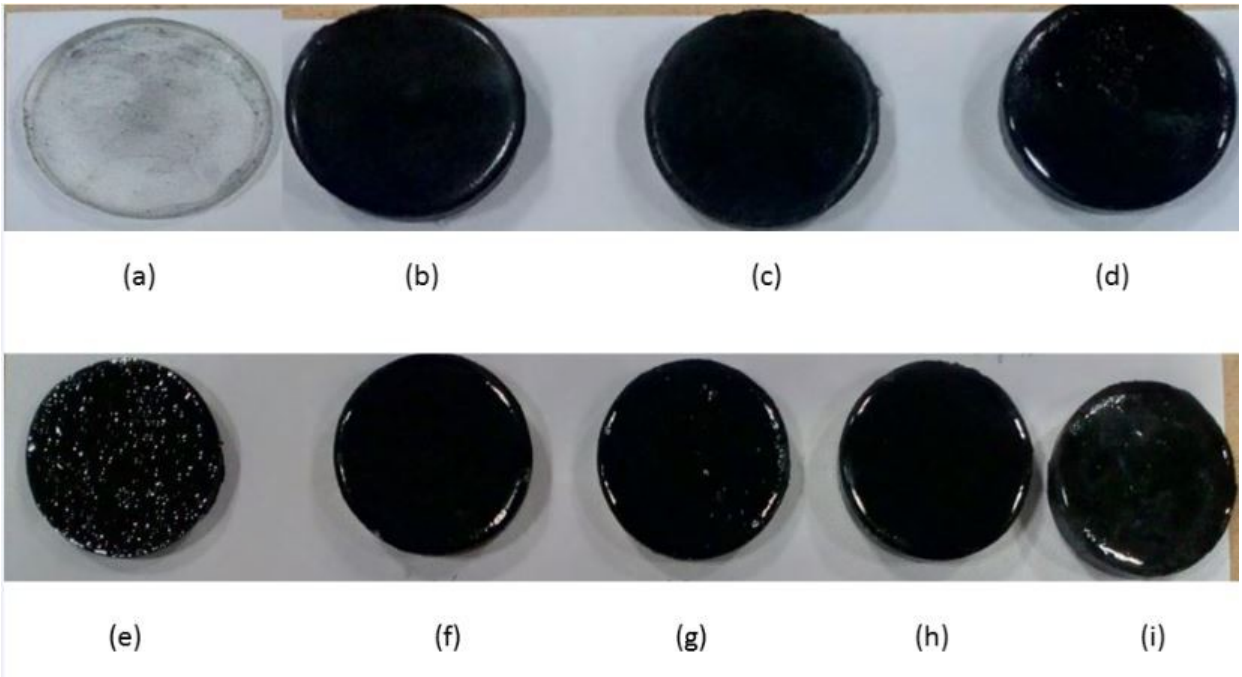

Figure 3.10 (a) L1 composite sample (b) L2 composite sample (c) L3 composite sample (d) L4 composite sample (e) L5 composite sample (f) L6 composite sample (g) L7 composite sample (h) L8 composite sample (i) L9 composite sample.

By varying the epoxy to hardener ratio, and weight percentage of RHA and GSA powder, 9 different composite samples are prepared according to the L9 Taguchi array as shown by Table 3.2 and their surface roughness is measured:

Table 3.2 L9 Array according to Design Of Experiments

S.NO.	EPOXY:HARDENER	WT.% OF RHA	WT.% OF GSA	SURFACE ROUGHNESS (µm)
1	5:3	0	0	1.97
2	5:3	4	4	2.27
3	5:3	8	8	2.96
4	2:1	0	4	1.87
5	2:1	4	8	2.14
6	2:1	8	0	2.02
7	3:1	0	8	1.94
8	3:1	4	0	1.66
9	3:1	8	4	2.17

While Table 3.2 shows the epoxy to hardener ratio and weight percentage of the reinforcement, Table 3.3 gives the composition of each of the 9 composites fabricated.

Table 3.3 Composition of the composites fabricated

S.NO.	EPOXY (gm)	HARDENER(gm)	RHA added (gm)	GSA added (gm)
L1	5	3	0	0
L2	11.5	6.9	0.8	0.8
L3	10.5	6.3	1.6	1.6
L4	6.4	3.2	0	0.4
L5	5.86	2.93	0.4	0.8
L6	6.12	3.06	0.8	0
L7	6.9	2.3	0	0.8
L8	7.2	2.4	0.4	0
L9	6.6	2.2	0.8	0.4

3.3.5 Wear Test

Ball-on-flat reciprocating tribometer was used to perform the test. Composites were cut in a 3cm x 3cm dimension. The counterbody was a 6mm steel ball [104]. A load of 9N was applied at frequency of 6 Hz as well as stroke of 1mm [105]. The experiments were done in room

temperature. The four composites upon which the wear test was done are depicted in figure 3.11.

Figure 3.11 (a) Sample L1 without reinforcement, (b) Sample L3 with both RHA and GSA as reinforcements, (c) Sample L4 with GSA as reinforcement, (d) Sample L6 with RHA as reinforcement

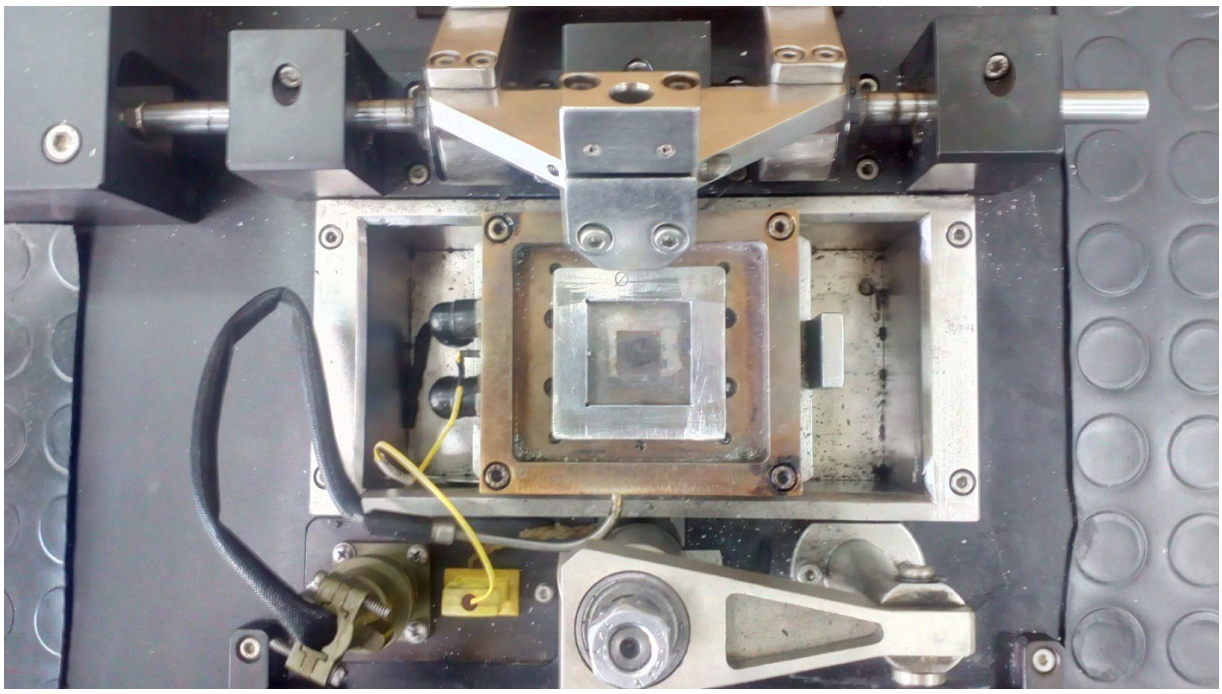

Figure 3.12 Ball on Flat Reciprocating Tribometer (Top View)

Figure 3.13 Ball on Flat Reciprocating Tribometer (Front View)

Figure 3.14 Steel Ball counter bodies

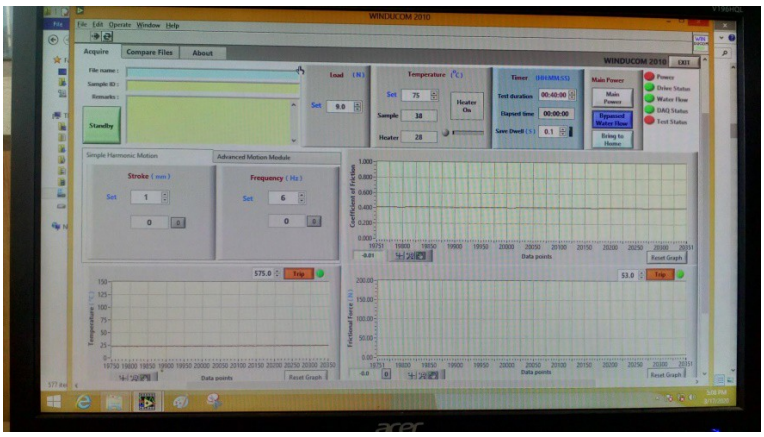

Figure 3.15 Software Display screen from where Ball-on-Flat Tribometer is controlled

Figure 3.12 and figure 3.13 give the top view and front view of the ball on flat tribometer respectively. Figure 3.14 shows the steel balls which were used to form the counter-body and perform the wear on epoxy composite samples. Figure 3.15 is the screenshot of the software used to analyze the wear on the composite samples. It shows all the conditions at which the wear test was performed like frequency, stroke, temperature.

CHAPTER 4

RESULTS AND ANALYSIS

4.1 Prediction of response variable for Delrin

It was found that the least mean square error while predicting both MRR as well as SR was obtained by NN. The mean square error obtained, for each regression technique is represented in table 4.1 given below. As can be seen from the table, neural net gives the best overall results, as it has an extremely small MSE.

Table 4.1 Mean square error obtained for response variable using various regression techniques

	MEAN SQUARE ERROR
Linear Regression	0.46
Support Vector Regression	2.15
KNN regression	0.275
Bayesian Ridge	1.981
Decision Tree regression	0.647
Gradient Boosting regression	0.86
Neural networks	0.108

The above results can be confirmed by visualizing the values obtained using regression techniques with the true values of both MRR and SR on two different graphs (The graph for neural network has not been included as the values for NN have been reshaped and will have to be represented by another scale than shown below) given by figure 4.1 and figure 4.2.

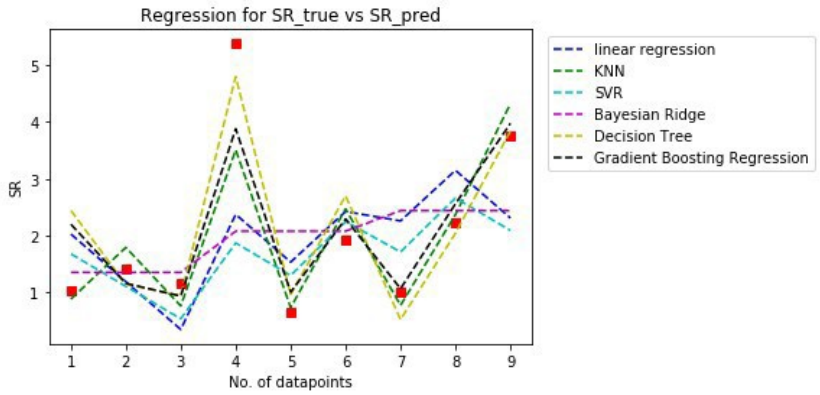

Figure 4.1 Obtained and true values of surface roughness

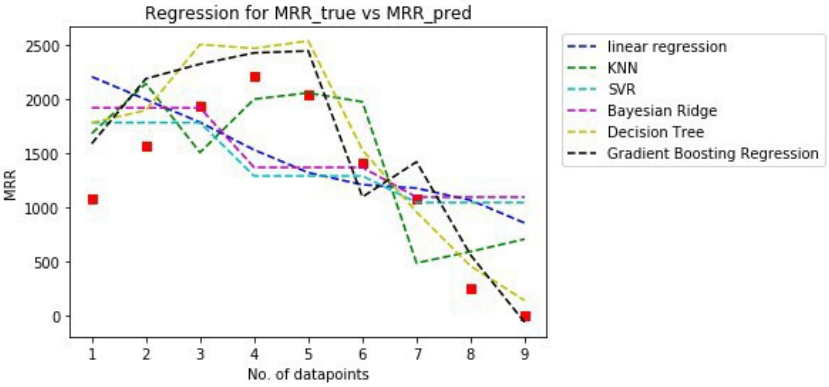

Figure 4.2 Obtained and true values of material removal rate

Out of the three regressions, viz, linear, SVR and Bayesian Ridge regression, linear regression has the least error for both MRR and SR. For linear regression the equation found is :

y =[[0.0092381 -1.31666667 -1.15333333] [-6.41442733 - 886.39633333 -65.8162]]* x + [1.4800000000000002 3380.573266666667].

4.2 Optimization of response variables for Delrin using GA

The equation obtained on application of linear regression was taken and Genetic Algorithm (GA) was applied to it for optimizing the input variables. In order to implement GA, the Optimization Toolbox in MATLAB was used. In this experiment, the MATLAB genetic algorithm was selected in the optimization toolbox. The following parameters are used during the optimization: An initial Population of 50 with feasible population as the function, and tournament type with a crossover of 0.8. We also selected a single point crossover and Mutation which is Adaptive Feasible.

As can be seen from figure 4.3 and figure 4.5, the multi-objective GA iterates for obtaining the best solution and finds it on the 139th generation. The graph in figure 4.4 plots Objective 2 on the y-axis against Objective 1 on the x-axis giving the Pareto front. These graphs help us determine the optimized solutions. Table 4.2 shows the optimized values of response variables obtained for optimized values of input variables.

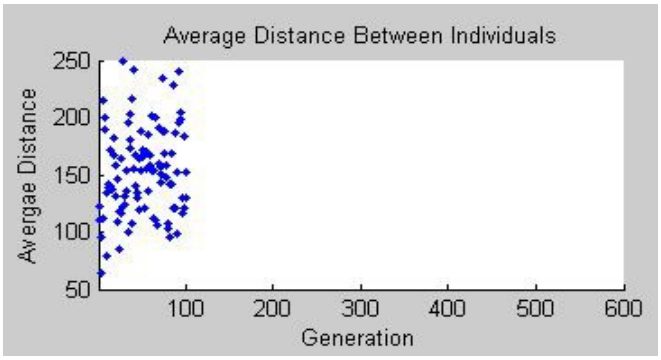

Figure 4.3 Average distance

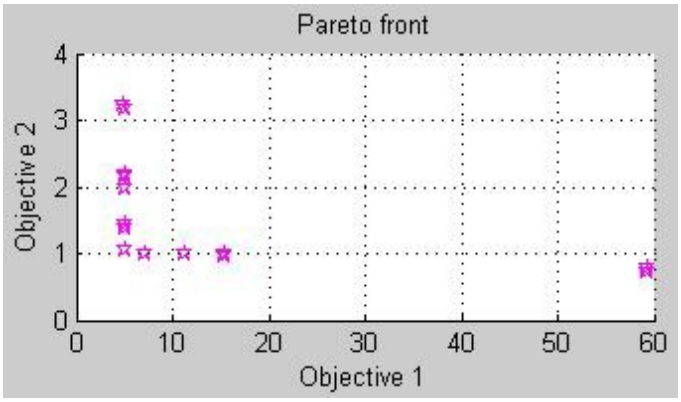

Figure 4.4 Pareto front graph

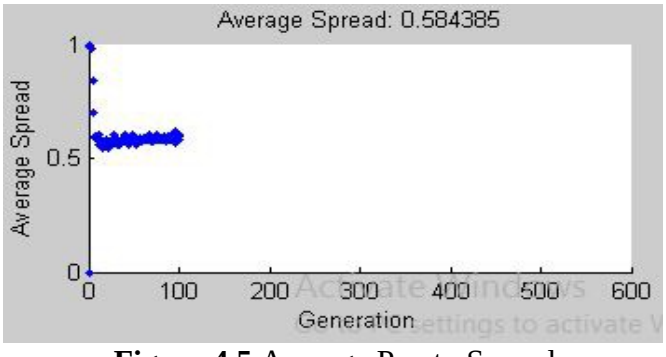

Figure 4.5 Average Pareto Spread

Table 4.2 Response variables optimized using Genetic Algorithm

Response Variables	No of generations	Optimal Response variable value	Optimal Speed value (rpm)	Optimal feed value (mm/rev)	Optimal Depth of Cut value (mm)
SR	139	0.351 micrometers	150	0.60	1.49
MRR	139	1788.91mm^3/min	150	0.60	1.49

These days one area where polymers are replacing metal based composites is sporting equipment. Both thermoplastic and thermosetting polymers are being investigated for that purpose. In this thesis we have found the response variables like surface roughness and for the thermoplastic polymer Delrin and optimized these parameters for a given set of inputs. We have also fabricated natural fiber reinforced epoxy composites and optimized the same response variables as in the previous case and then compared the two results.

4.3 Optimization of response variables for Delrin using RSM

Apart from utilizing genetic algorithm to optimize the response variables, we used the Response Surface Methodology (RSM) method with a view to confirm the results obtained by genetic algorithm. Figure 4.6 gives us the optimized results for the response variables using RSM. According to RSM the optimized value of SR is 0.736 micrometers and optimized value of MRR is 2436 mm^3/min. These optimized values of response variables were obtained at input values of 192.424 rpm of speed, 0.458 mm/rev of feed and 1.5 mm of depth of cut. These results closely agree with the results obtained using genetic algorithm.

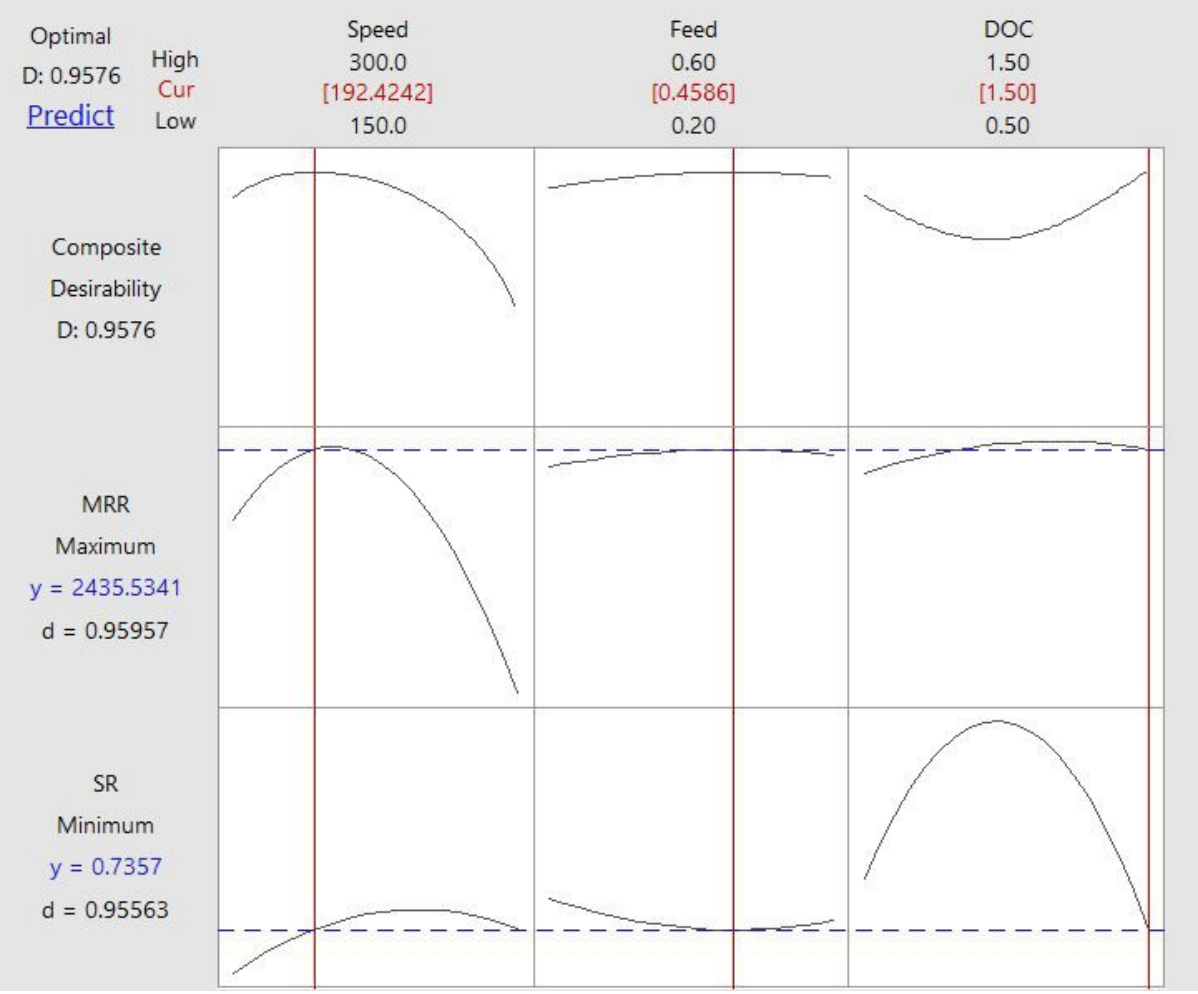

Figure 4.6 Optimized results for response variables using RSM

4.4 ANOVA of factors in CNC turning of Delrin rod

Taguchi method is used to figure out the best values of the input factors for the least value of the surface roughness. ANOVA helps us determine the percentage contribution of each factor. For surface roughness the response table for means has been given by table 4.3. The response table helps us select the best value of each input factor. For surface roughness the input factors have been selected using smaller-the-better criterion. Figure 4.7 gives the main effects plot for means for the output variable surface roughness.

Table 4.3 Response Table for Means

Level	Speed	Feed	DOC
1	1.1644	2.2667	1.8489
2	2.3733	1.8556	3.3111
3	2.4356	1.8511	0.8133
Delta	1.2711	0.4156	2.4978
Rank	2	3	1

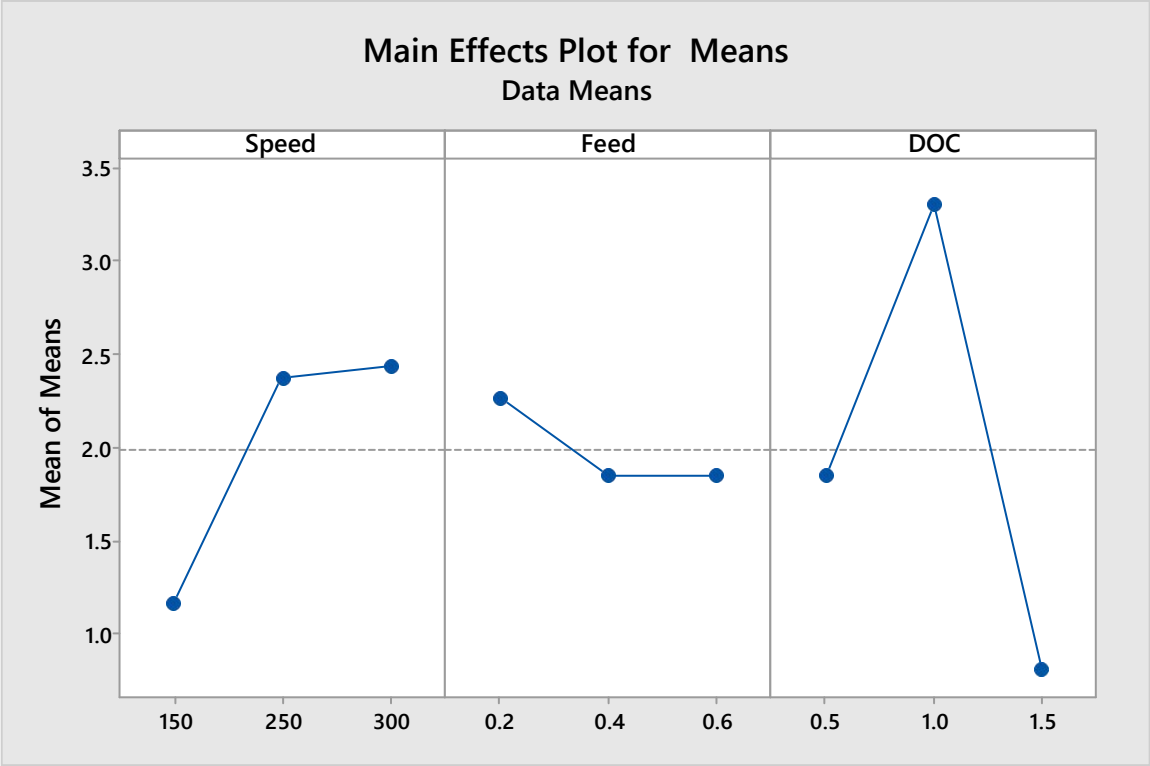

Figure 4.7 Main effects plot for means for surface roughness

Similar to the response table for means is the response table for signal-to-noise ratio. It is given by table 4.4. Figure 4.8 give the graph for the main effects plot for SN Ratio for the output variable surface roughness.

Table 4.4 Response Table for Signal to Noise Ratios (Smaller is better)

Level	Speed	Feed	DOC
1	-0.6606	-4.4635	-4.5869
2	-5.2969	-3.6712	-9.4635
3	-6.0096	-3.8325	2.0832
Delta	5.3490	0.7923	11.5467
Rank	2	3	1

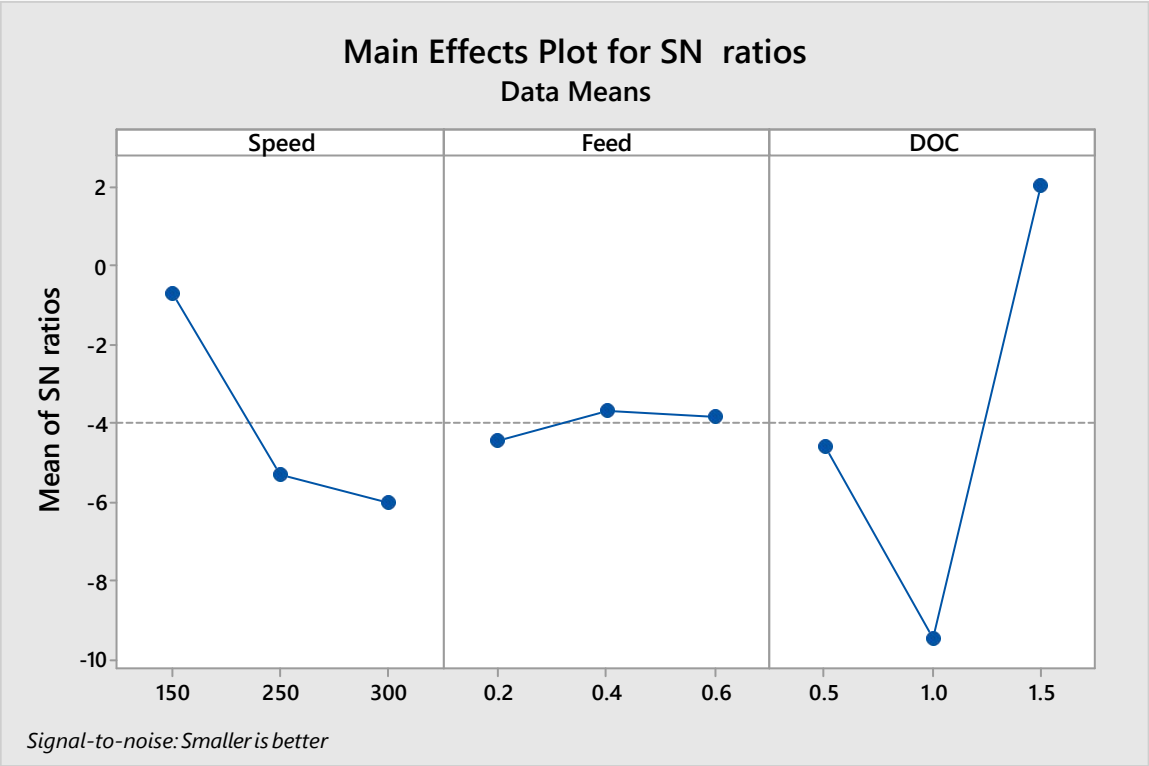

Figure 4.8 Main effects plot for SN Ratio for surface roughness

Main effects plot of means as well as S/N Ratio are depicted using figure 4.7 as well as figure 4.8 respectively. These graphs show that the optimized result is A1B3C3, that is, for a speed of 150 rpm, feed of 0.6 mm/rev and depth of cut of 1.5 mm the least surface roughness is obtained. These values closely agree with those obtained from other optimization techniques.

Table 4.5 Analysis of Variance for SR

Source	DF	Adj SS	Adj MS	F	P	Percentage Contribution
Speed	2	9.243	4.6215	8.81	0.002	18.82
Feed	2	1.025	0.5126	0.98	0.394	2.087
DOC	2	28.348	14.1740	27.01	0.000	57.72
Total		49.111				

Table 4.5 displays the ANOVA for the surface roughness response variable of Delrin rod. The analysis of variance gives the sum of squares (SS), degrees of freedom (DF), F-values (F-VAL.), mean square (MS) in addition to probability value (PVAL.) as well as percentage influence exerted by each factor. Since the significance level or p-value of 2 input parameters is less than 0.05, those factors are significant. However, for feed the p-value is more than 0.05 and thus it is statistically insignificant. Depth of cut has proven to be the most significant factor accounting for 57.72% of the effect on the surface roughness

in the machining operation.

4.5 Prediction of response variable of epoxy composite samples

Various regression techniques have been used to determine or predict the response variable values (in this case surface roughness). Table 4.6 gives the mean square error obtained for each regression technique while predicting surface roughness for given inputs.

Table 4.6 Mean square error obtained for response variable using various regression techniques

	MEAN SQUARE ERROR
Linear Regression	0.049
Support Vector Regression	0.062
KNN regression	0.064
Bayesian Ridge	0.098
Decision Tree regression	0.089
Gradient Boosting regression	0.172

The above results can be confirmed by visualizing the values obtained using regression techniques with the true values of SR as shown by the figure 4.9.

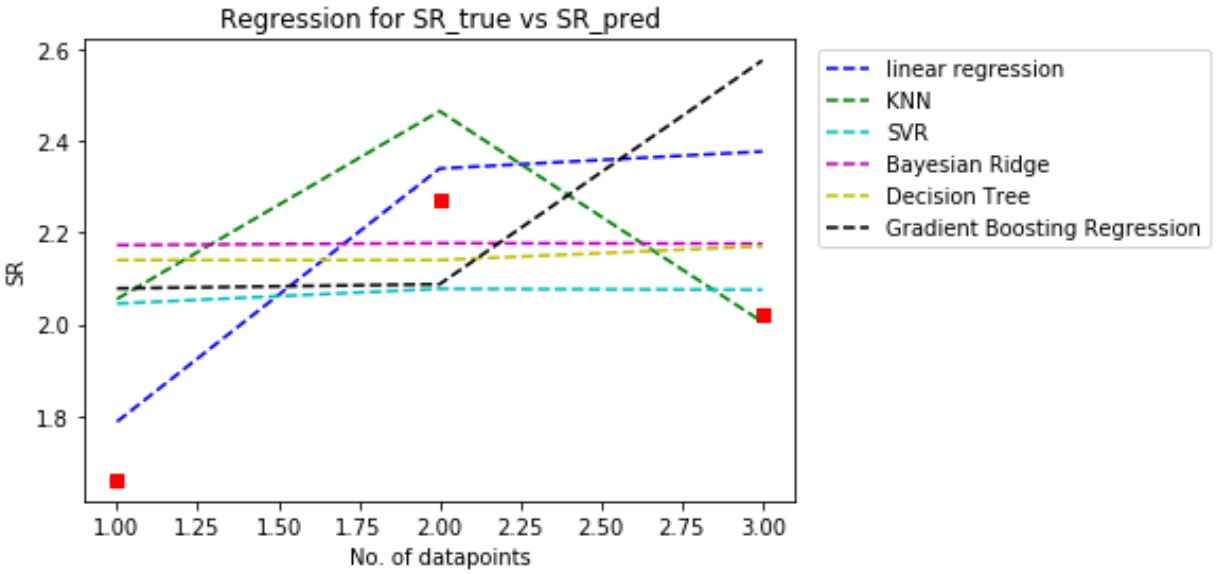

Figure 4.9 Graphical comparison between true values and predicted values of surface roughness for various regression techniques

4.6 Optimization of response variable of epoxy composite using GA

Linear regression has the least mean square error, that is, it most closely agrees with the graph and is the line of best fit. Our next step is to implement Genetic Algorithm (GA). For that we will need the function equation. Since linear regression shows the least mean square error, it's equation is chosen. The equation describing the curve of linear regression is:

$$y = [-0.30191146 \;\; 7.19537106 \;\; 3.77478414] * x + 2.40508229446753$$

Genetic Algorithm is implemented using the Optimization Toolbox in Matlab. Before carrying out the optimization we need to select the initial population. In our implementation, the initial population has been selected as 50 which is the default value. Out of this initial population, the ones selected "to be passed on" are chosen via a 'tournament type' selection criteria. Moreover, the mutation type chosen is 'Adaptive Feasible'.

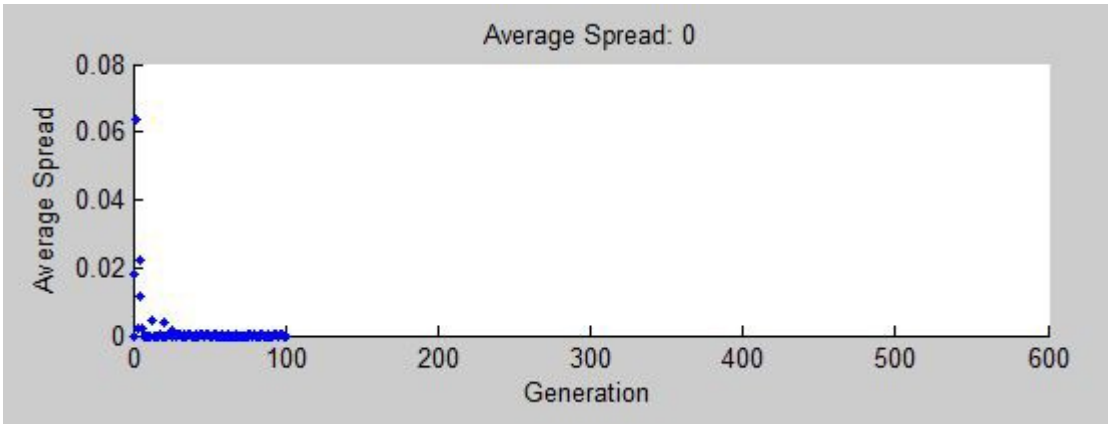

Figure 4.10 Average Pareto Spread

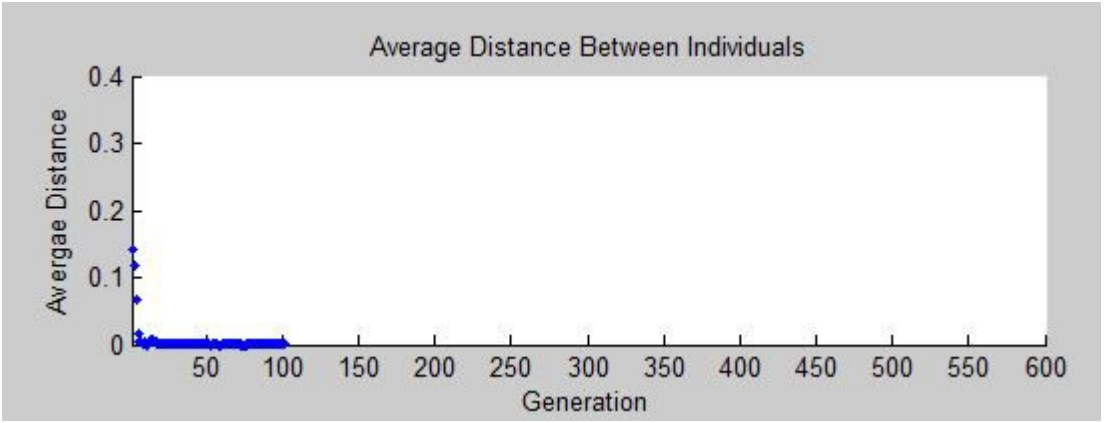

Figure 4.11 Average Distance between individuals

Figures 4.10 and 4.11 give the average Pareto spread and average distance between individuals and show that optimization took just a 102 generations to achieve which is quite fast. Table 4.7 gives the optimized value of the response variable using genetic algorithm.

Table 4.7 Response variables optimized using Genetic Algorithm

Response Variable	No of generations	Optimal Response variable value	Optimal Epoxy:Hardener ratio	Optimal Wt% of RHA	Optimal Wt% of GSA
SR	102	1.503 micrometers	2.99:1	0	0

4.7 Optimization of response variable of epoxy composite using RSM

Apart from utilizing genetic algorithm to optimize the response variables, we used the Response Surface Methodology (RSM) method with a view to confirm the results obtained by genetic algorithm. Figure 4.12 gives us the optimized results for the response variables using RSM. According to RSM the optimized value of SR is 1.3903 micrometers. These optimized values of response variables were obtained at input values of 2.4761:1 epoxy: hardener ratio, 1.9 weight percentage of RHA and 0 weight percentage of GSA. These results closely agree with the results obtained using genetic algorithm.

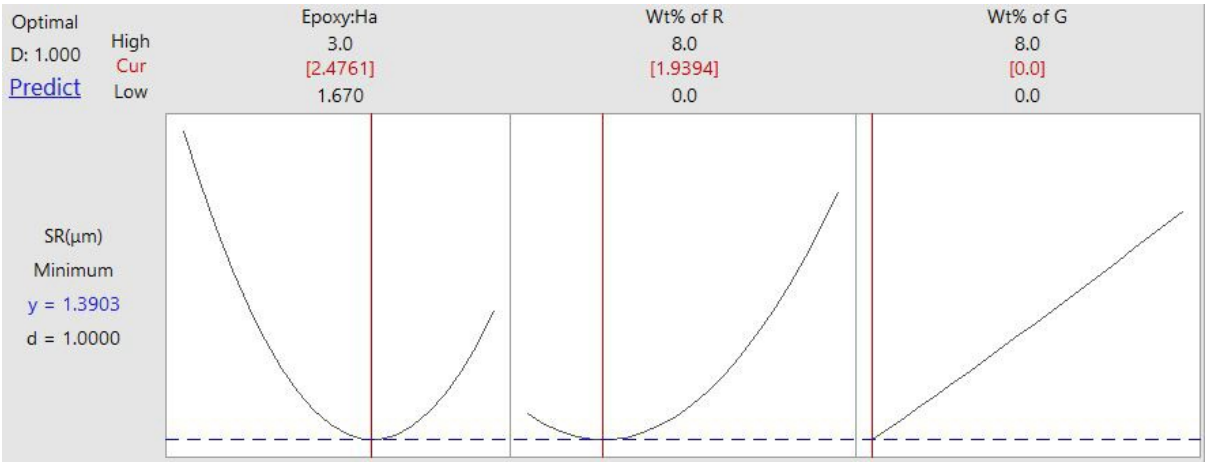

Figure 4.12 Optimized results for response variables using RSM

4.8 ANOVA of factors in epoxy composite samples

Taguchi method is used to figure out the best values of the input factors for the least value of the surface roughness. ANOVA helps us determine the percentage contribution of each factor. For surface roughness the response table for means has been given by table 4.8. The response table helps us select the best value of each input factor. For surface roughness the input factors have been selected using smaller-the-better criterion. Figure 4.13 gives the main effects plot for means for the output variable surface roughness.

Table 4.8 Response Table for Means

Level	Epoxy:Hardener	Wt% of RHA	Wt% of GSA
1	2.4	1.927	1.883
2	2.01	2.023	2.103
3	1.923	2.383	2.347
Delta	0.477	0.457	0.463
Rank	1	3	2

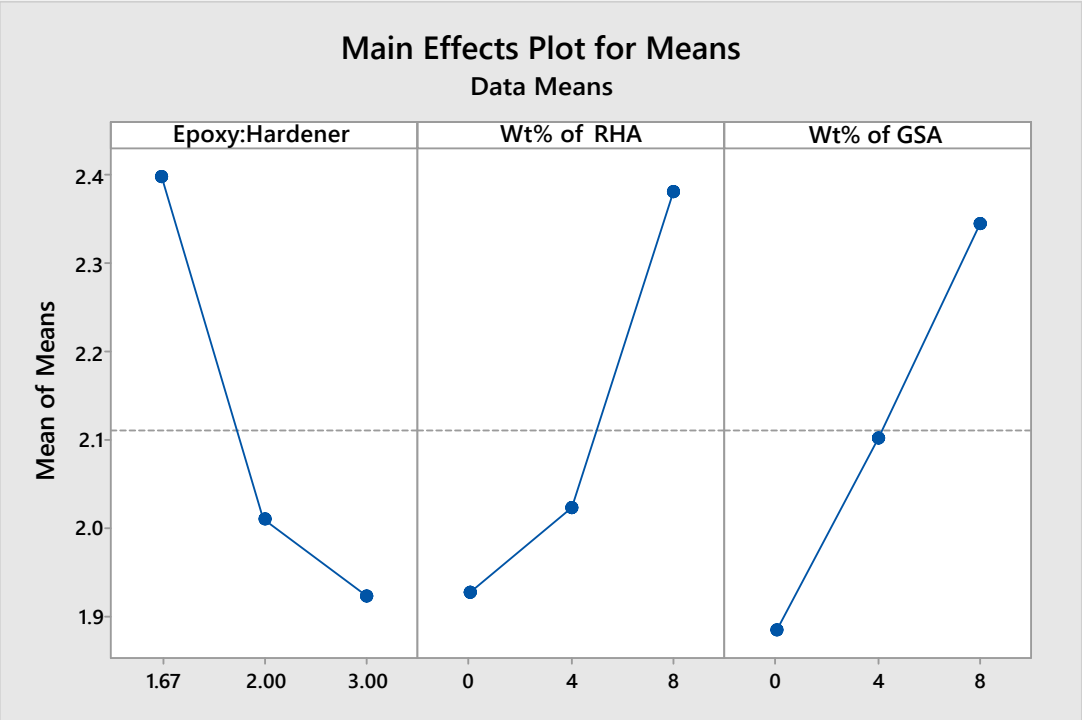

Figure 4.13 Main effects plot for Means

Similar to the response table for means is the response table for signal-to-noise ratio. It is given by table 4.9. Figure 4.14 give the graph for the main effects plot for SN Ratio for the output variable surface roughness.

Table 4.9 Response Table for Signal to Noise Ratios (Smaller is better)

Level	Epoxy:Hardener	Wt% of RHA	Wt% of GSA
1	-7.479	-5.694	-5.466
2	-6.051	-6.044	-6.429
3	-5.629	-7.421	-7.263
Delta	1.849	1.727	1.797
Rank	1	3	2

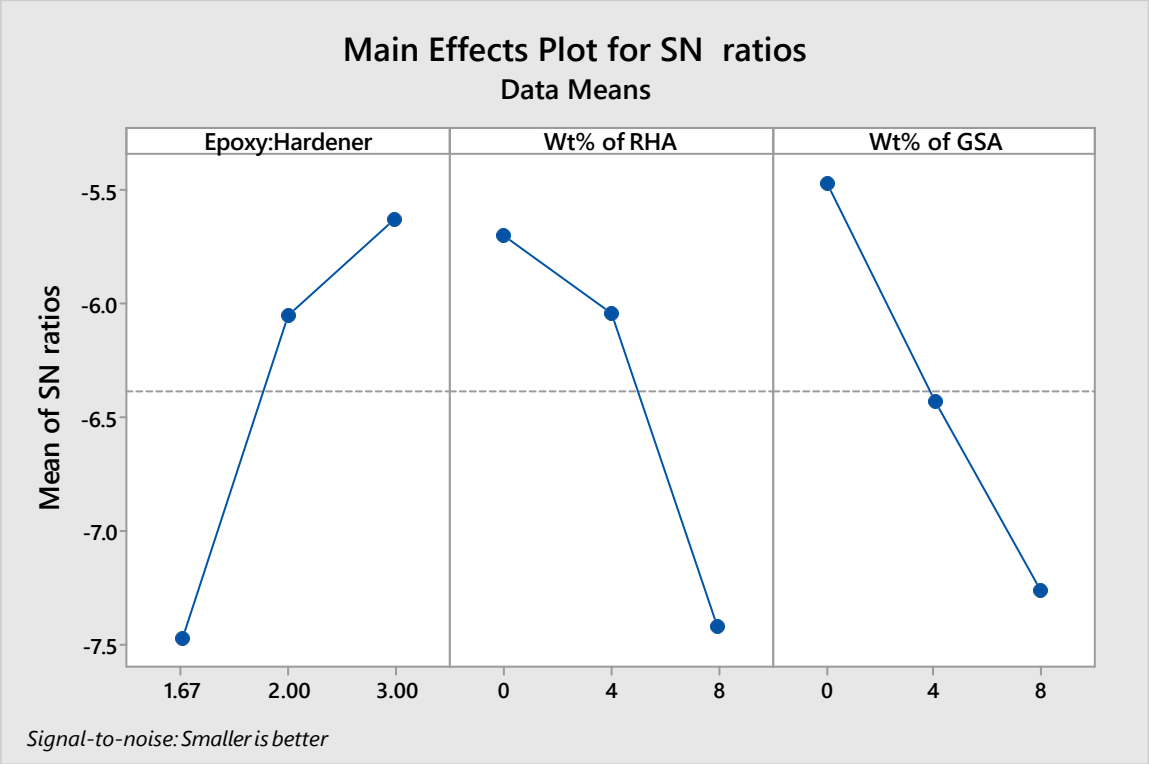

Figure 4.14 Main effects plot for S/N Ratio

Main effects plot of means as well as S/N Ratio are depicted using figure 4.13 as well as figure 4.14 respectively. These graphs show that the optimized result is A3B1C1, that is, for an epoxy: hardener ratio of 3 and without the addition of any reinforcements the least surface roughness is obtained. This result closely agrees with that obtained using GA.

Table 4.10 Analysis of Variance for SR

Source	DF	Seq SS	Adj SS	Adj MS	F	P	Percentage Contribution
Epoxy:Hardener	2	5.6369	5.63686	2.81843	363.14	0.003	36.35464231
Wt% of RHA	2	4.9997	4.99966	2.49983	322.09	0.003	32.24531125
Wt% of GSA	2	4.8532	4.85316	2.42658	312.66	0.003	31.30046694
Residual Error	2	0.0155	0.01552	0.00776			
Total	8	15.5052					

Table 4.10 displays the ANOVA for the surface roughness response variable. The analysis of variance gives the sum of squares (SS), degrees of freedom (DF), F-values (F-VAL.), mean square (MS) in addition to probability value (PVAL.) as well as percentage influence exerted by each factor. Since the significance level or p-value of all 3 input parameters is less than 0.05, all 3 input variables are statistically significant.

4.9 Abrasive Wear analysis of epoxy composite samples

To determine the specific wear rate, we will first have to calculate the volume loss. The volume loss is found by dividing weight loss with density of composite. Weight loss is observed from the digital weight balance by weighing the sample before and after the wear test has been performed on it. Once the volume loss is found we then find the specific wear rate with the formula:

$$\mathbf{W_s = V/(L \times D)}$$

Here W_s is used to show specific rate of wear with units of mm^3/Nm, V is the loss in volume in mm^3, L stands for load applied on the sample which is equal to 9N and D is the stroke length in mm and its value is 1mm. Table 4.11 gives the dimensions of the samples upon which wear analysis was done in addition to the wear rate and the volume loss.

Table 4.11 Abrasive Wear rate of samples

S.No.	Sample No.	Area (cm^2)	Height (cm)	Volume loss (mm^3)	Wear rate (mm^3/Nm)
1	L1	9	0.8	1.467	163
2	L3	9	0.7	0.586	65.11
3	L4	9	0.5	1.060	117.77
4	L6	9	0.5	0.785	87.22

4.9.1 Ball-on-Flat Tribometer Wear test for sample L1

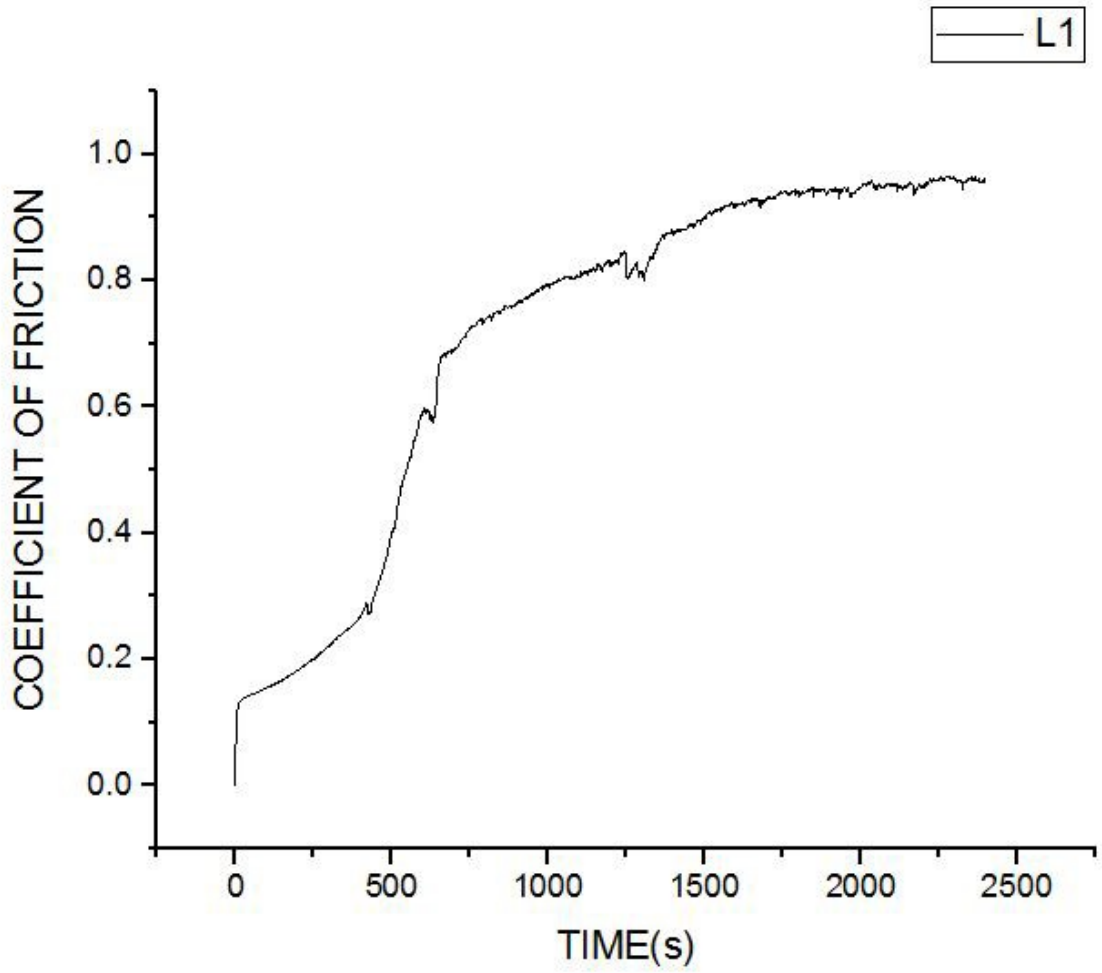

Figure 4.15 Coefficient of Friction vs Time graph of sample L1

From Figure 4.15 it can be observed that the coefficient of friction (COF) increases in direct proportion to time up to a peak limit and then it saturates.

The average value of COF is determined to be 0.71.

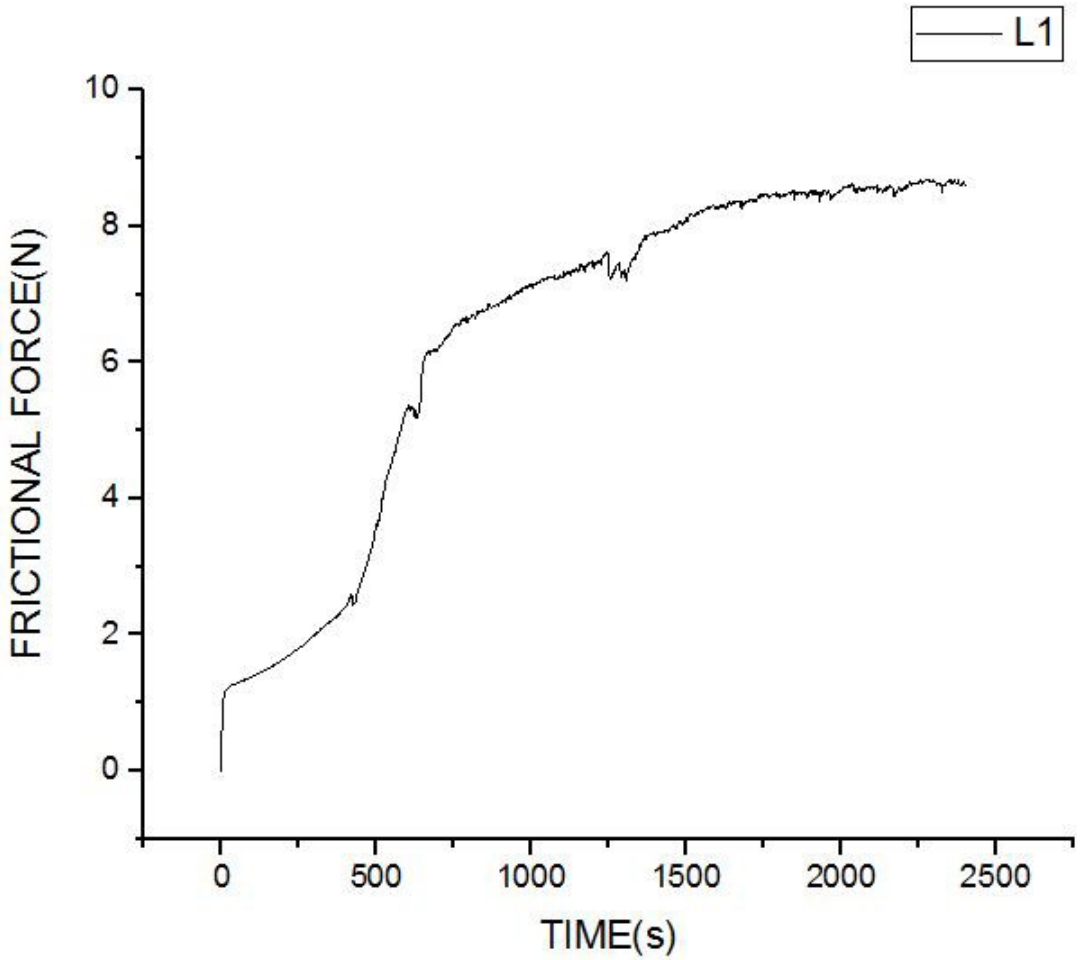

Figure 4.16 Frictional Force vs Time graph of sample L1

As we can see from figure 4.16, the value of frictional force rises with time and then reaches a plateau.

The Frictional Force average value was observed to be about 6.43 N.

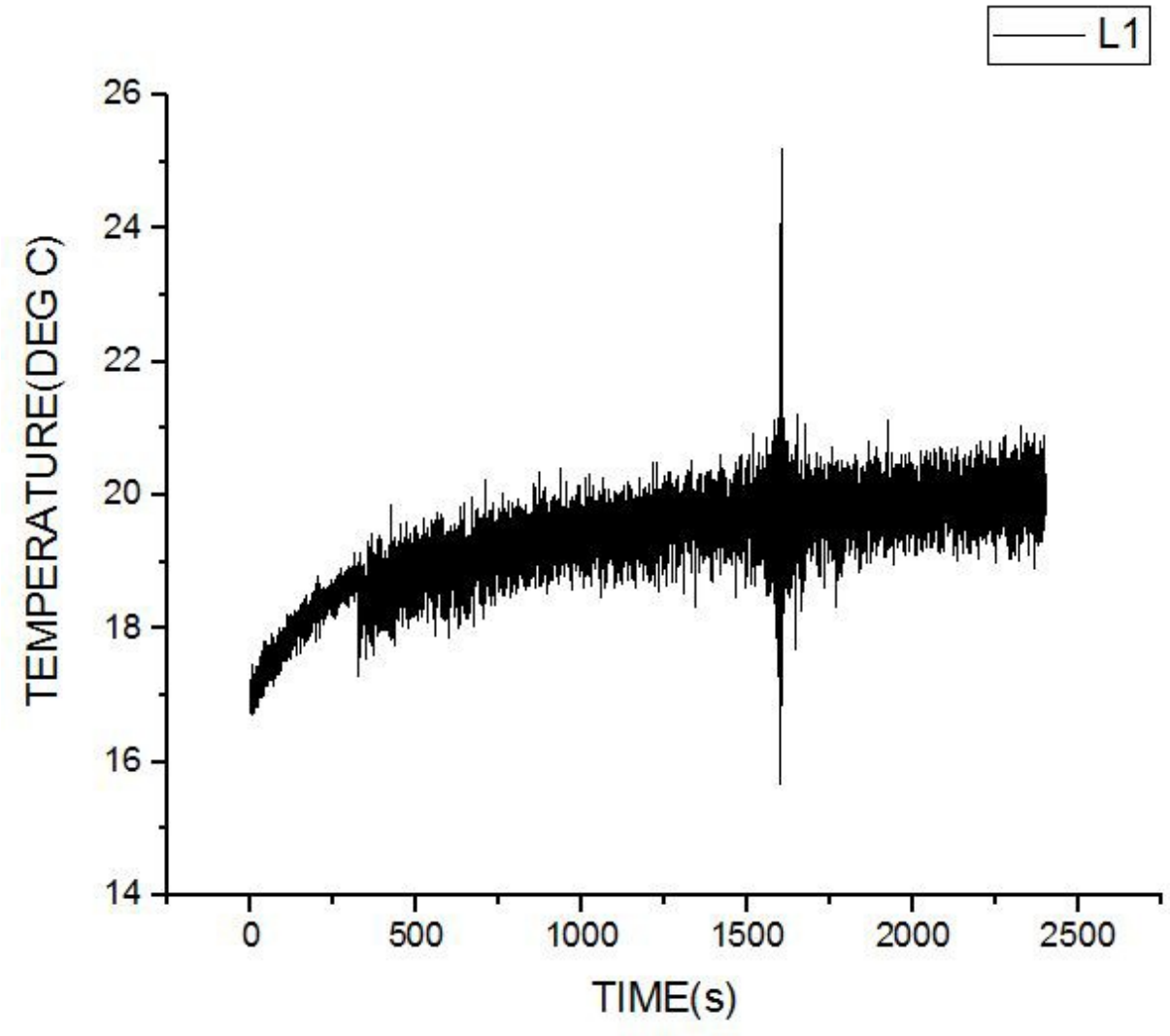

Figure 4.17 Temperature vs Time graph of Sample L1

From figure 4.17, it is observed that temperature measurements indicate a temperature of 16.86 degree Celsius at the start of wear test.

The average temperature reading registered for the duration of the test is about 19.32 degrees Celsius.

4.9.2 Ball-on-Flat Tribometer Wear test for sample L3

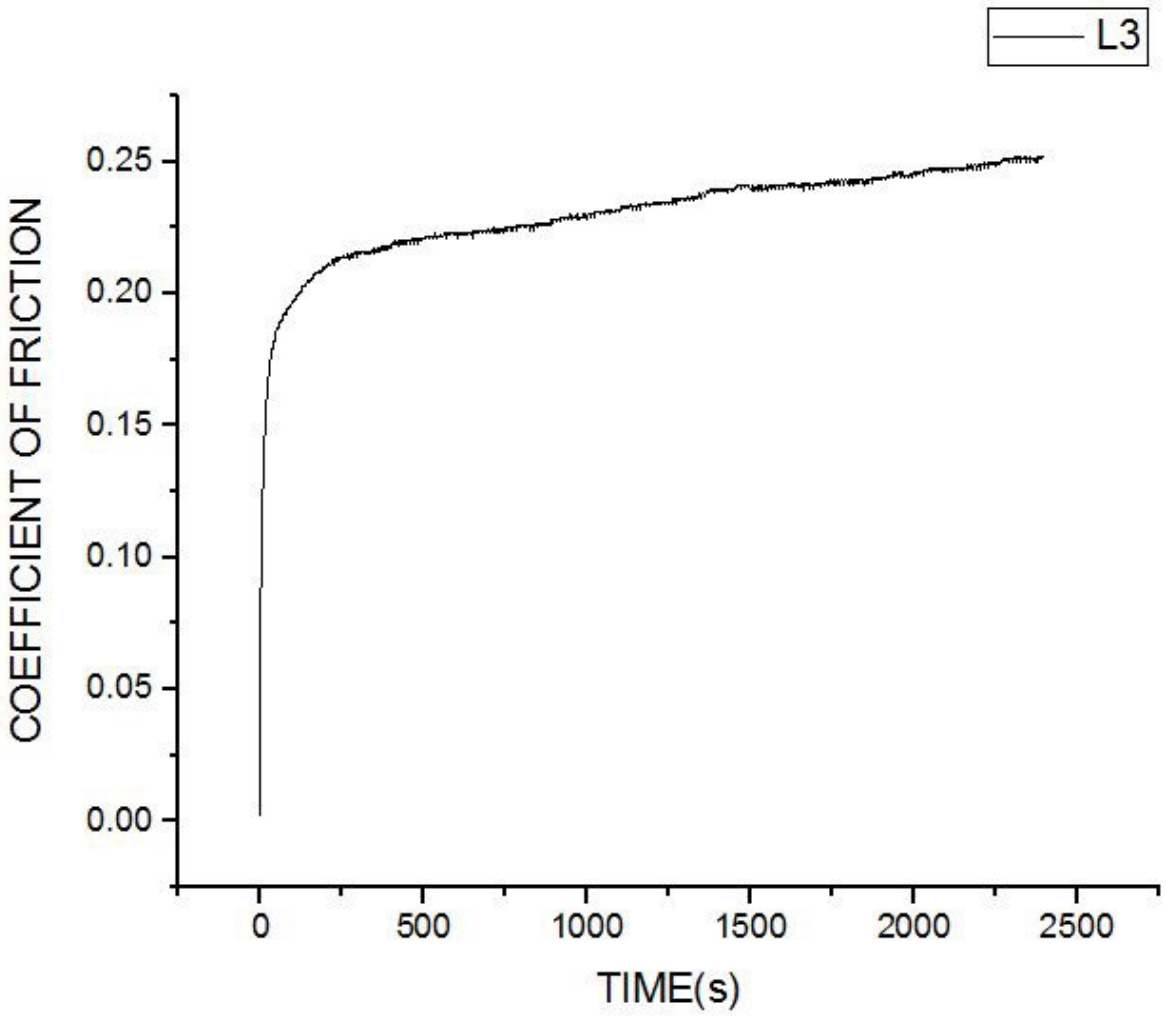

Figure 4.18 Coefficient of Friction vs Time graph of sample L3

As can be seen from Figure 4.18 the coefficient of friction (COF) increases in direct proportion to time up to a peak limit and then it saturates.

The average value of COF is determined to be 0.23.

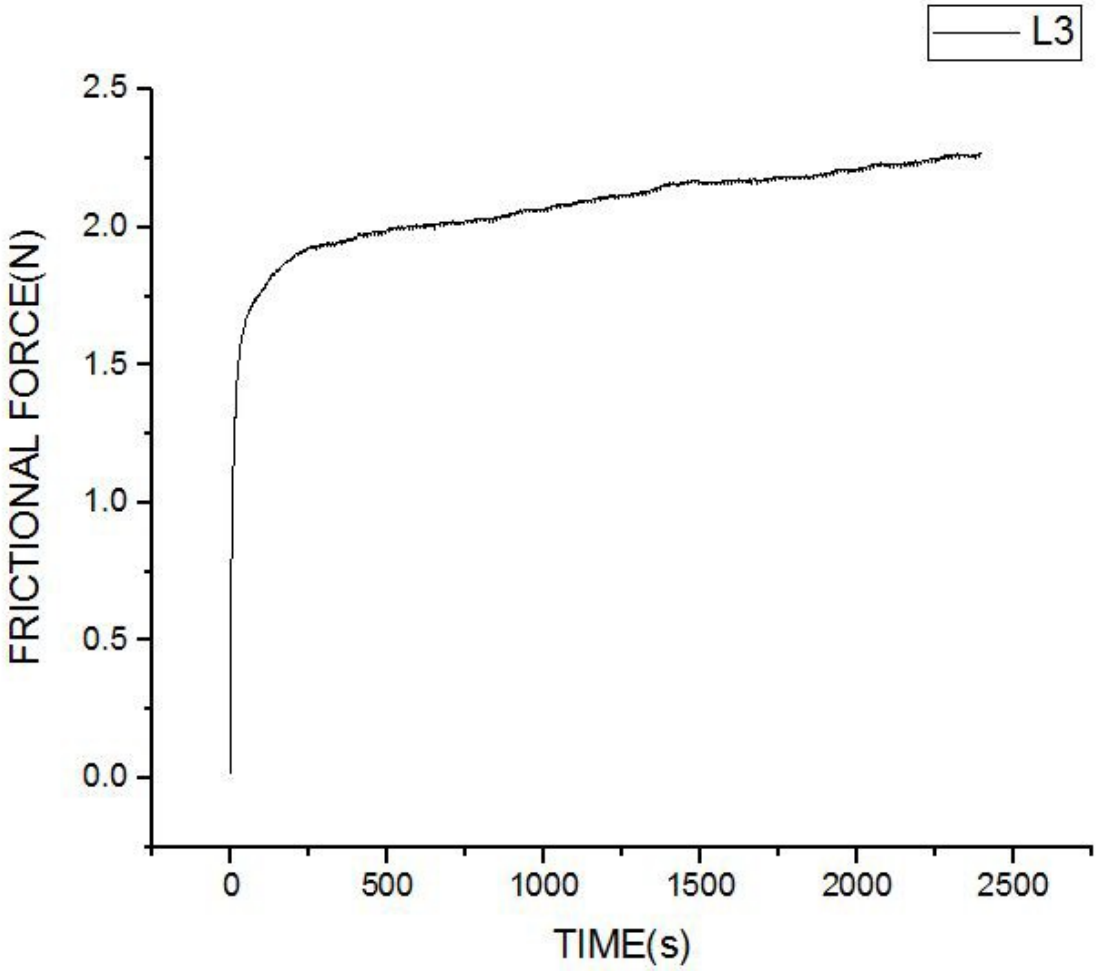

Figure 4.19 Frictional Force vs Time graph of sample L3

As we can see from figure 4.19, the value of frictional force rises with time and then reaches a plateau.

The Frictional Force average value is observed to be about 2.07 N.

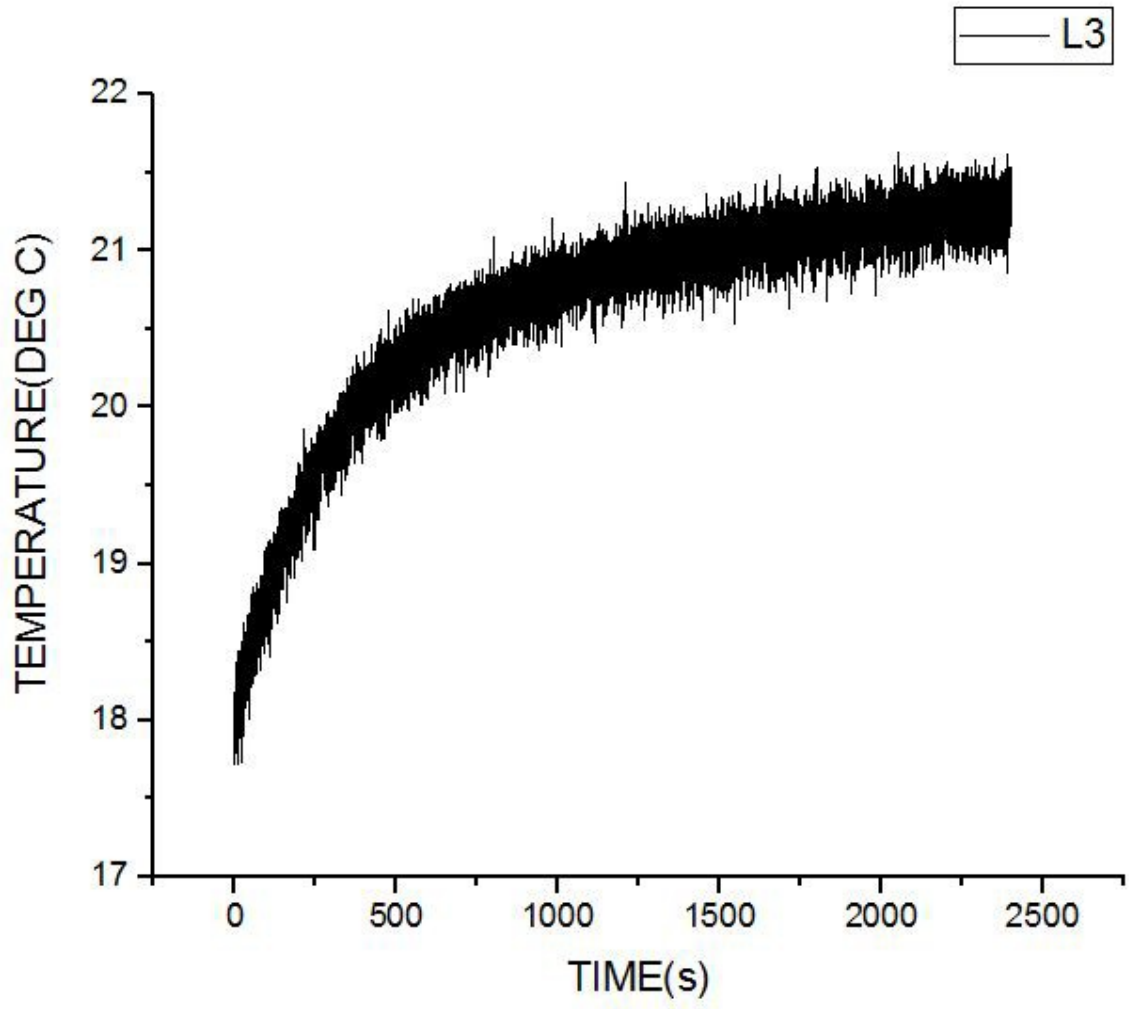

Figure 4.20 Temperature vs Time graph of Sample L3

From figure 4.20, it is observed that temperature measurements indicate a temperature of 18.005 degrees Celsius at the start of wear test.

The average temperature reading registered for the duration of the test is about 19.32 degrees Celsius.

4.9.3 Ball-on-Flat Tribometer Wear test for sample L4

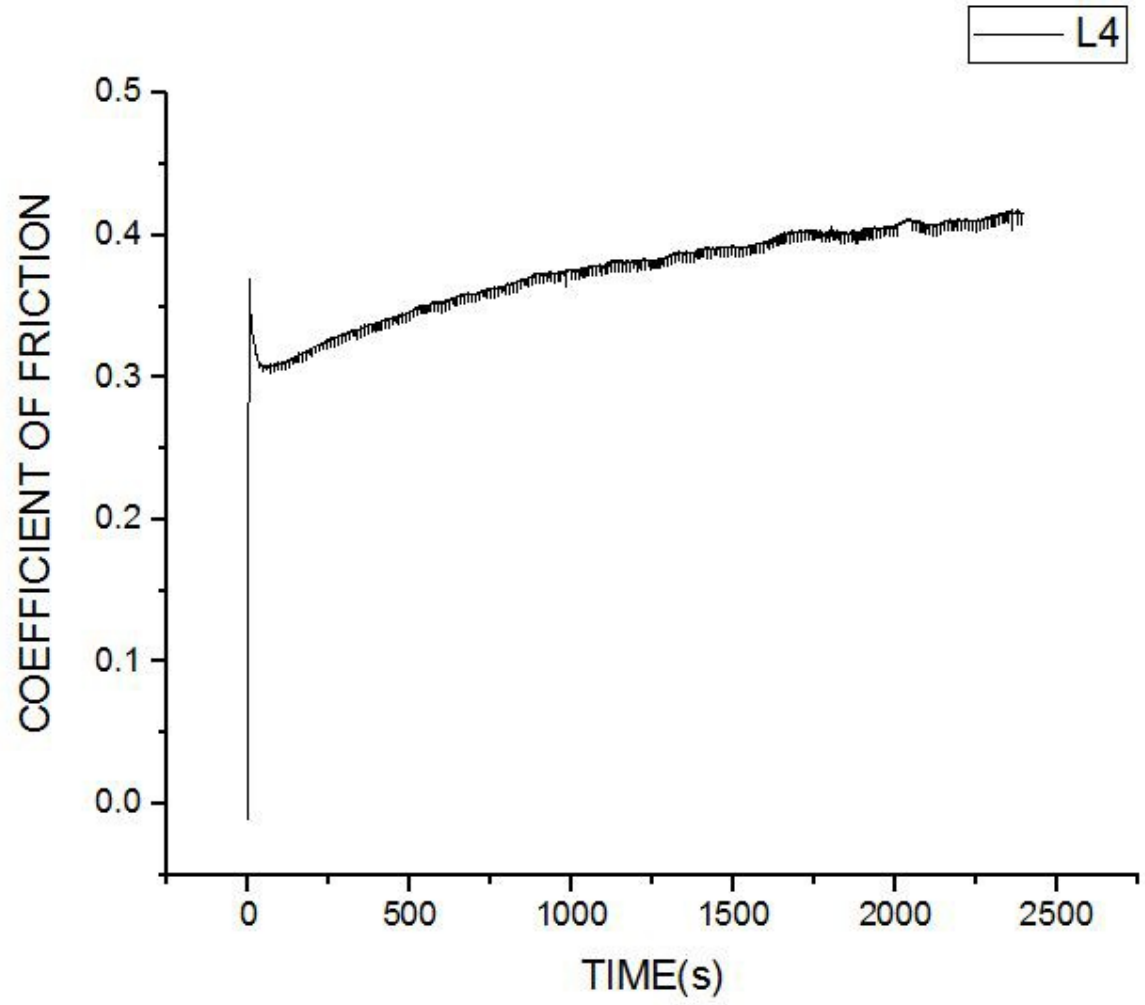

Figure 4.21 Coefficient of Friction vs Time graph of sample L4

From Figure 4.21 it was observed that the coefficient of friction (COF) increases in direct proportion to time up to a peak limit and then it saturates.

The average value of COF is determined to be 0.37.

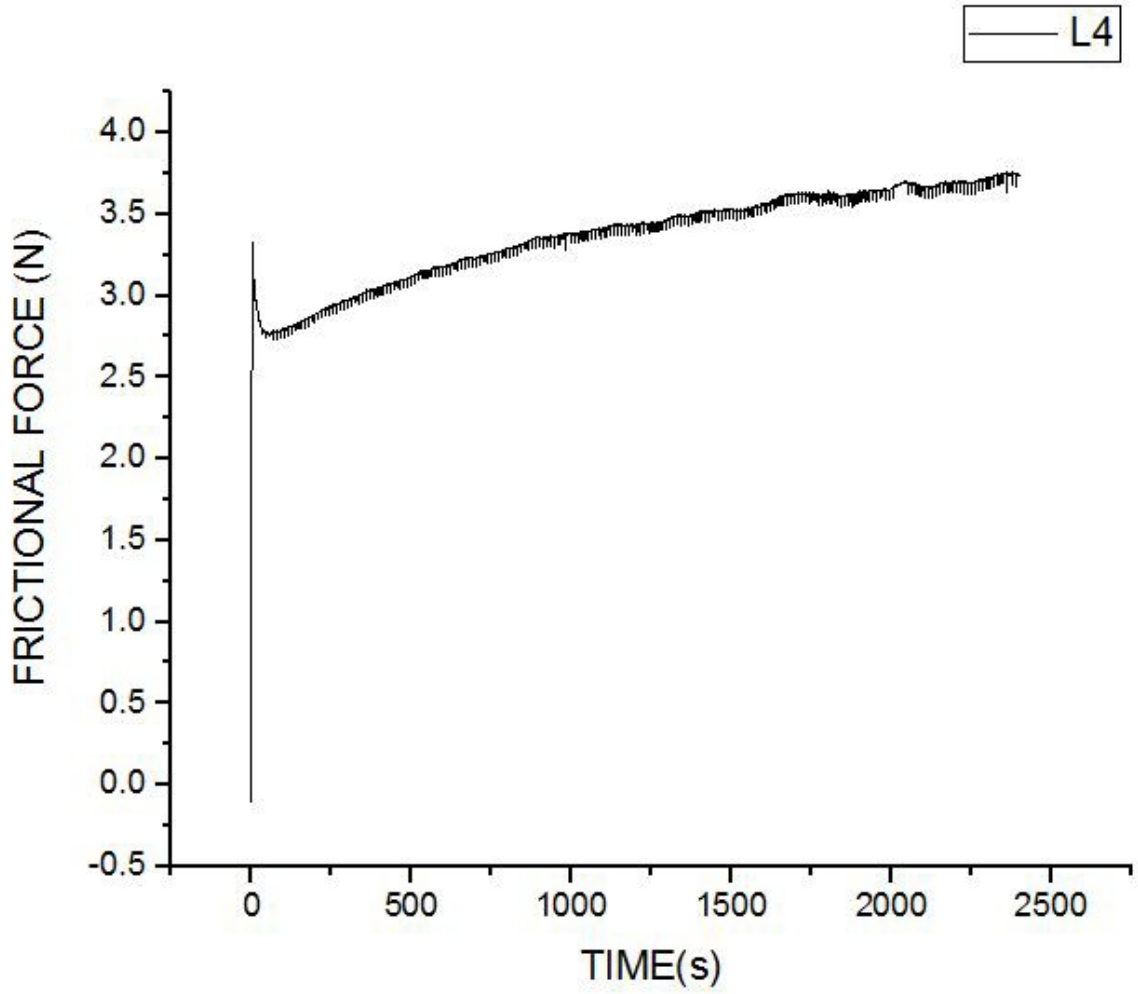

.

Figure 4.22 Frictional Force vs Time graph of sample L4

As we can see from figure 4.22, the value of frictional force rises with time and then reaches a plateau.

The Frictional Force average value was observed to be about 3.37 N.

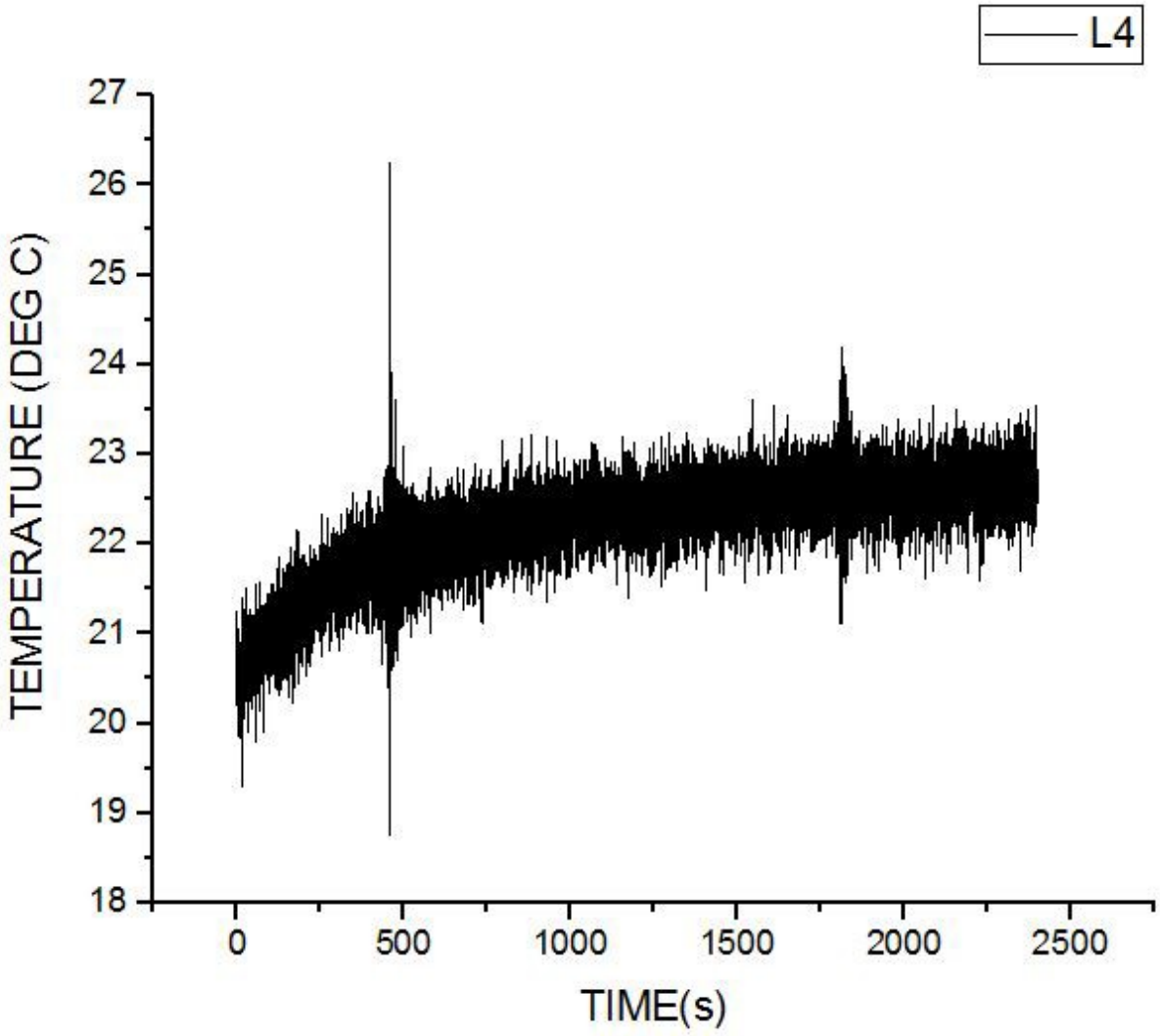

Figure 4.23 Temperature vs Time graph of Sample L4

From figure 4.23, it is observed that temperature measurements indicate a temperature of 20.548 degree Celsius at the start of wear test.

The average temperature reading registered for the duration of the test is about 22.21 degrees Celsius.

4.9.4 Graph obtained after wear test of sample L6

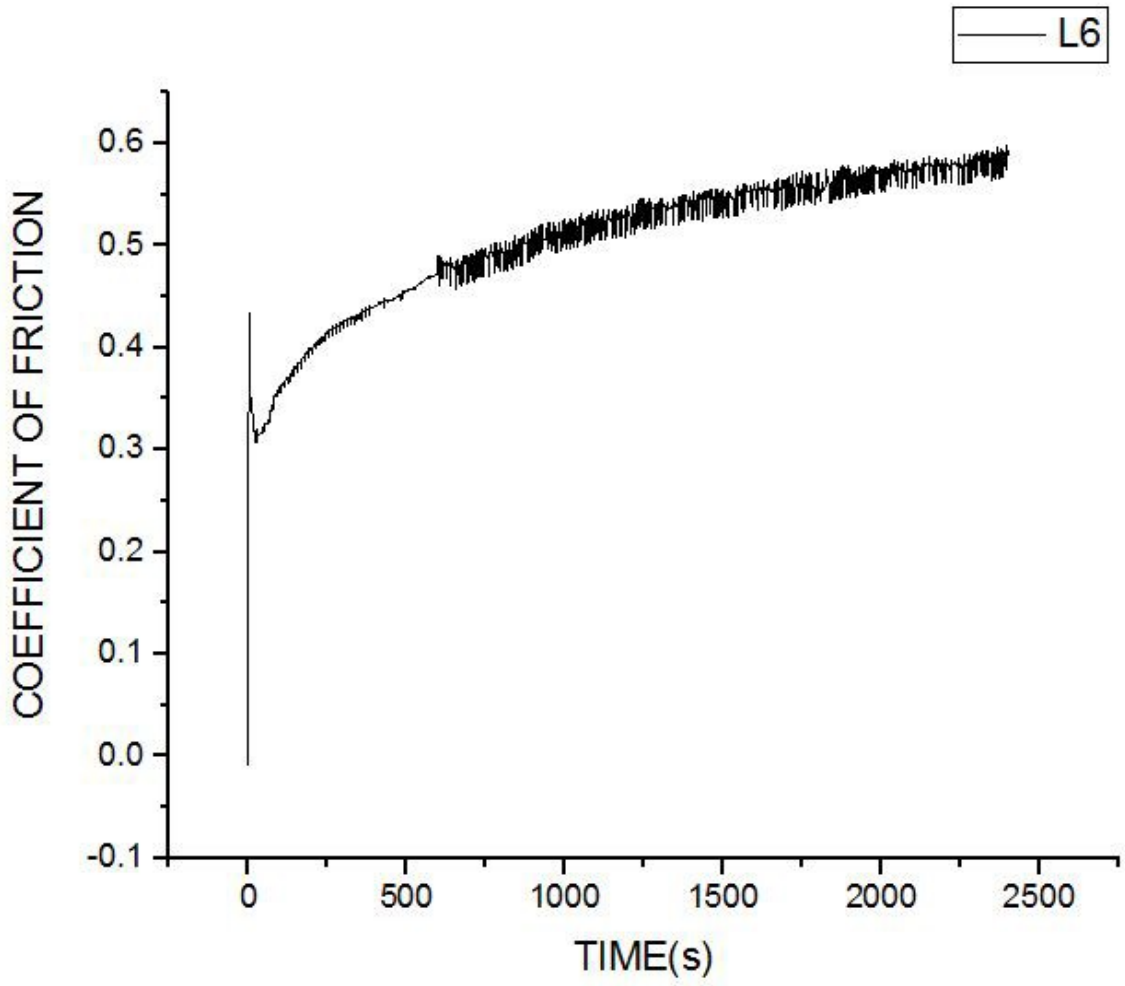

Figure 4.24 Coefficient of Friction vs Time graph of sample L6

From Figure 4.24 it was observed that the coefficient of friction (COF) increases in direct proportion to time upto a peak limit and then it saturates.

The average value of COF is determined to be 0.51.

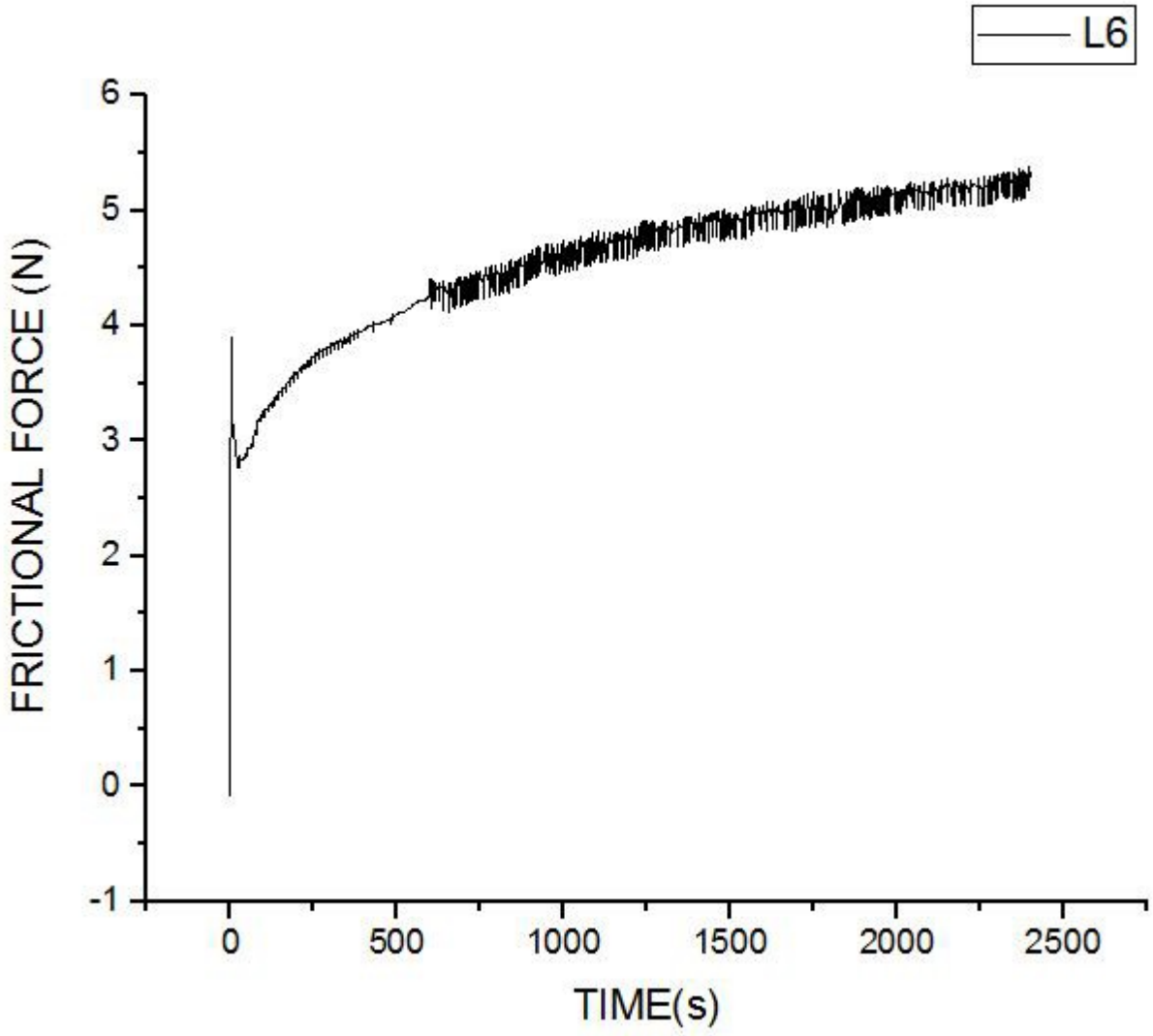

Figure 4.25 Frictional Force vs Time graph of sample L6

As we can see from the figure 4.25, the value of frictional force rises with time and then reaches a plateau.

The Frictional Force average value was observed to be about 4.57 N.

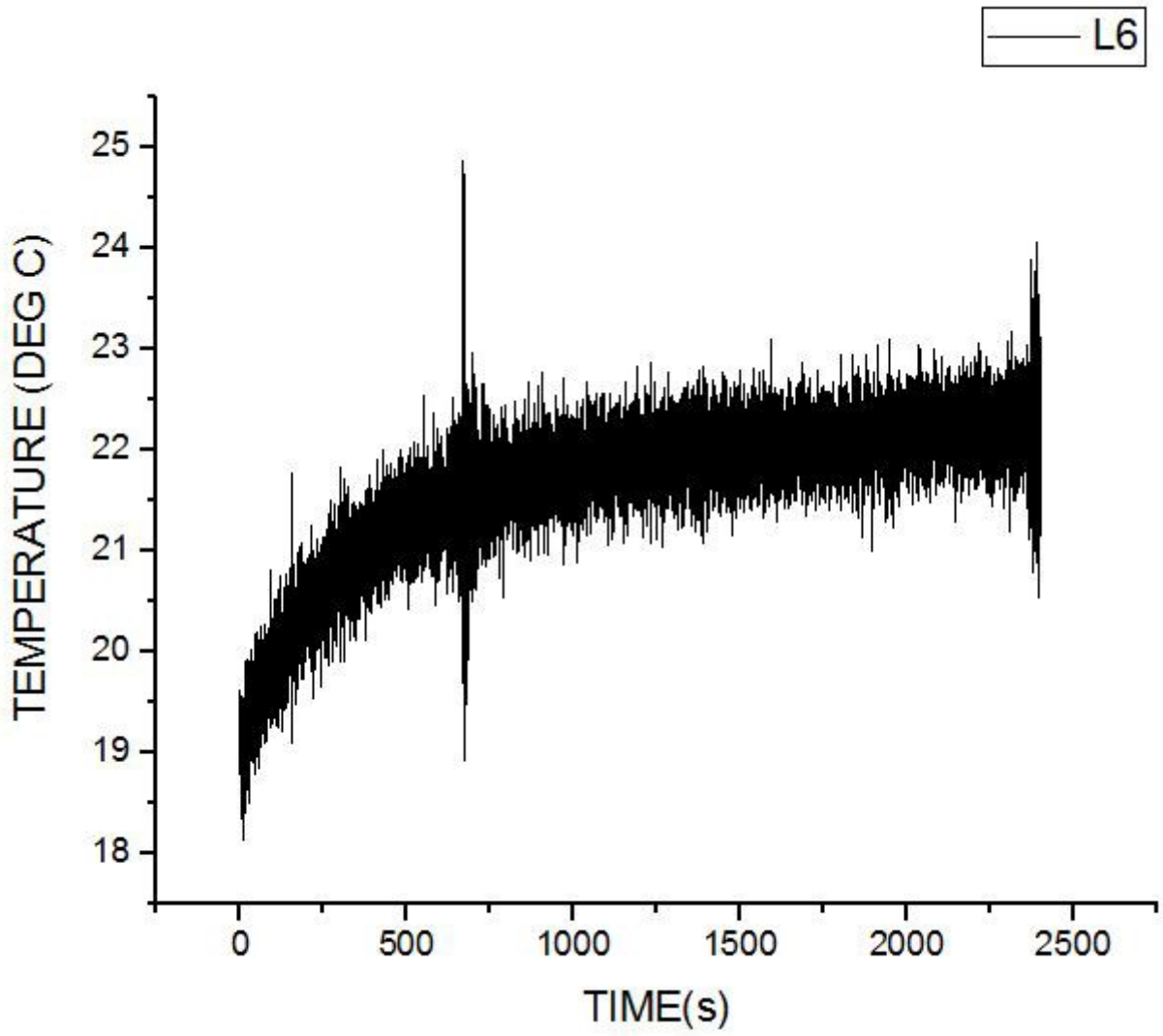

Figure 4.26 Temperature vs Time graph of Sample L6

From figure 4.26, it is observed that temperature measurements indicate a temperature of 19.625 degrees Celsius at the start of wear test.

The average temperature reading registered for the duration of the test is about 21.63 degrees Celsius.

4.9.5 Coefficient Of Friction For All 4 Composite Samples

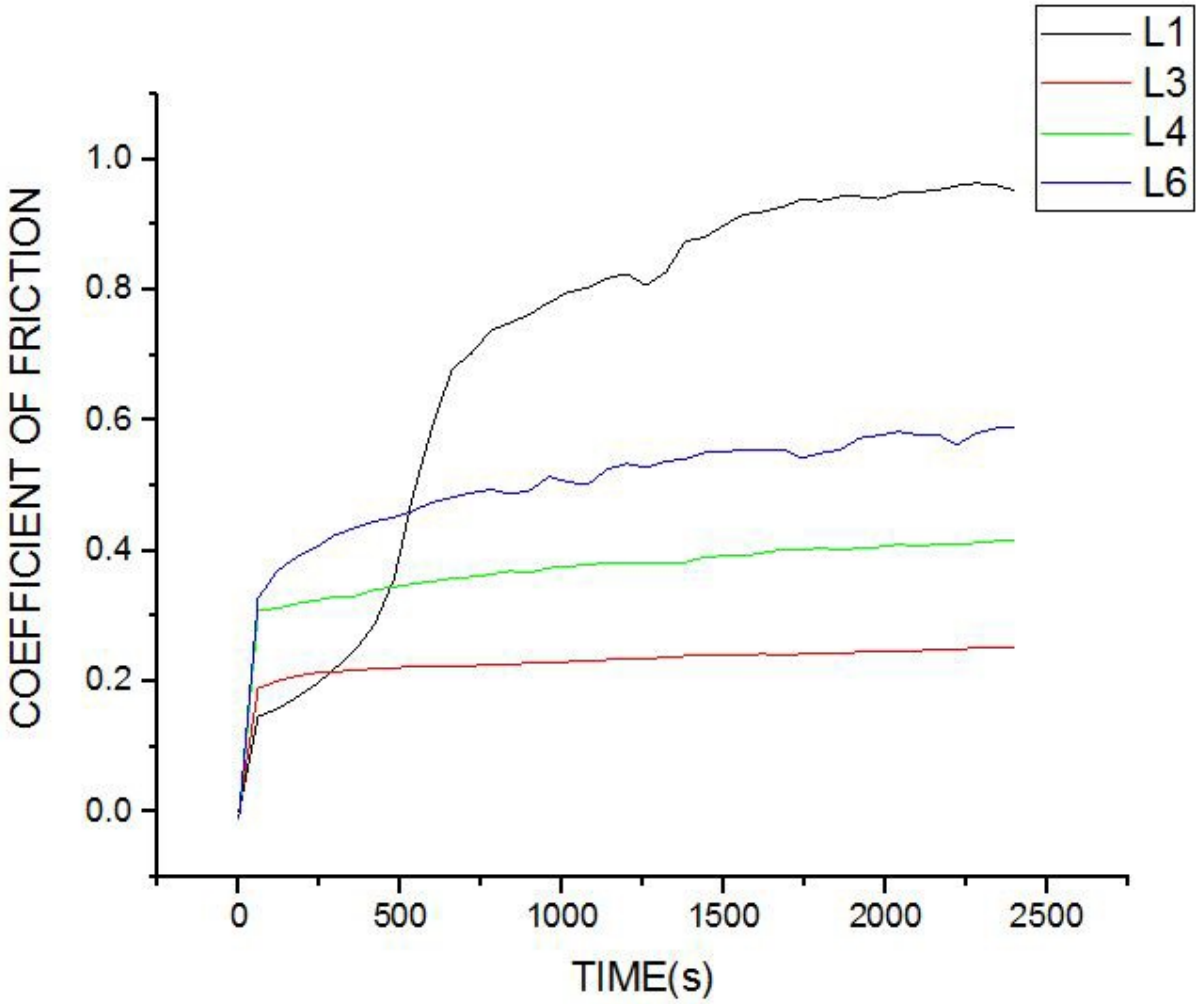

Figure 4.27 COF vs Time graph comparison for all 4 composite samples

Figure 4.27 compares the coefficient of friction of all 4 composite samples upon which wear test has been performed.

It has been found that L1 has the highest average value of coefficient of friction of 0.71. This is no doubt due to the fact that sample L1 has 0% reinforcement. Thus, sample L1 has the highest wear rate.

4.9.6 Frictional Force For All 4 Composite Samples

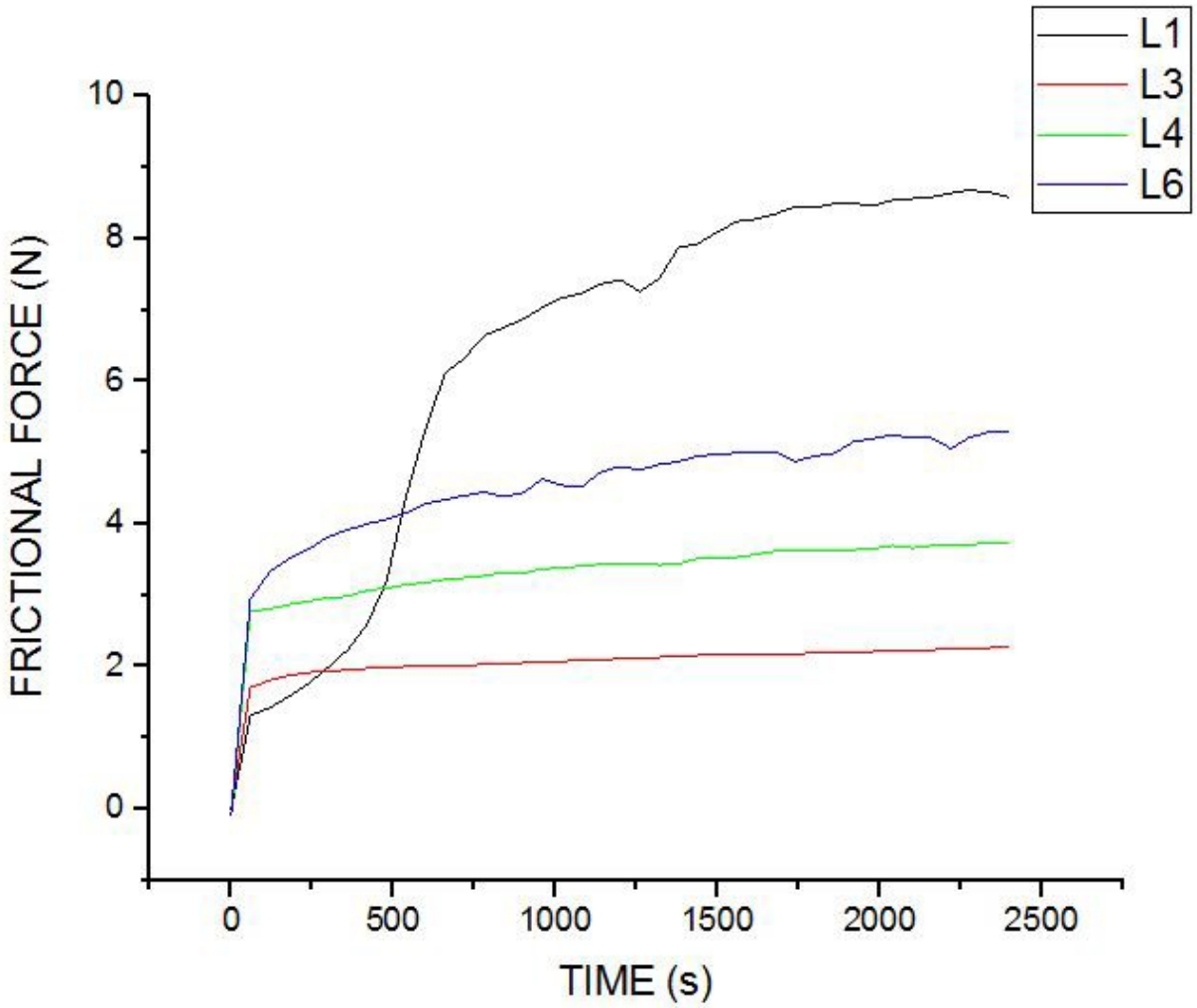

Figure 4.28 FF vs Time graph comparison for all 4 composite samples

Figure 4.28 compares the frictional force generated on all 4 composite samples upon which wear test has been performed.

It has been found that sample L1 generates the highest frictional force. Sample L1 has 0% reinforcement and therefore does not get the added benefit of load bearing compared to samples with some reinforcement.

CHAPTER 5

CONCLUSIONS

This thesis has fabricated Groundnut Shell Ash (GSA) and Rice Husk Ash (RHA) reinforced epoxy composites as well as optimized the surface roughness of the samples obtained. In addition to that, we have also optimized the response parameters of Delrin rod using genetic algorithm. This thesis helps come to the conclusions stated below:

- Out of all the regression techniques, neural networks give the least mean square error of 0.108 while predicting the response variable values for Delrin rod.
- Genetic algorithm (GA) was implemented to find optimum cutting parameters for Delrin rod and the values of the input variables were found to be 150 rpm speed, 0.6mm/rev feed and 1.49mm depth of cut. At this combination optimized value of SR is 0.351micrometre and MRR is 1788.91mm^3/min.
- GA gave an optimized result in 139 generations which is quite fast.
- Response surface methodology (RSM) was also used to optimize the response variable values and the value of SR thus obtained was 0.736 micrometers while it was 2436 mm^3/min for MRR. These optimized values of response variables were obtained at input values of 192.424 rpm of speed, 0.458 mm/rev of feed and 1.5 mm of depth of cut. These results closely agree with the results obtained using genetic algorithm.
- From the main effects plot we found that the optimized result is A1B3C3, that is, for a speed of 150 rpm, feed of 0.6 mm/rev and depth of cut of 1.5 mm the least surface roughness is obtained. These values closely agree with those obtained from other optimization techniques.
- ANOVA helps us determine the percentage contribution of each input factor and it was found that depth of cut is the most significant factor with a total contribution of 57.72%.
- The P-value of feed was found to be greater than 0.05 and thus it was found to be statistically insignificant.
- Natural fibers like GSA and RHA were used to reinforce Epoxy resin matrix successfully.
- Linear regression was found to have the least mean square error of 0.049 among all the regression techniques. Thus the curve obtained by linear regression is the line of best fit.

- The optimized result for minimizing the surface roughness was found by the implementation of the Genetic Algorithm (GA). For an epoxy to hardener mixture of 2.99 and without adding any reinforcement, a minimum surface roughness of 1.503μm was determined.
- The Genetic Algorithm optimization gave an optimized result in a 102 generations which is quite fast.
- Response surface methodology (RSM) was also used to optimize the response variable values and the value of SR thus obtained was 1.3903 micrometers. These optimized values of response variables were obtained at input values of 2.4761:1 epoxy: hardener ratio, 1.9 weight percentage of RHA and 0 weight percentage of GSA. These results closely agree with the results obtained using genetic algorithm.
- From the main effects plot it was found that the optimized result is A3B1C1, i.e., for an epoxy:hardener ratio of 3 and 0% addition of reinforcements, the minimum surface roughness is obtained. These values closely agree with those obtained from other optimization techniques.
- From the Analysis of variance it was found that all three input variables were statistically significant and that epoxy:hardener ratio was the most significant variable accounting for 36.35% of the total effect.
- Ball-on-flat tribometer was used to carry out wear analysis on the epoxy composite samples and it was found that the highest wear was found to be by sample L1, that is, the neat epoxy composite. It showed the highest volume loss of 1.467 mm^3 and a maximum wear rate of 163 mm^3/Nm. Thus, reinforcements made the composite more wear resistant.

5.1 Future Scope

This thesis looked at the optimization of surface roughness of natural fiber reinforced thermosetting composite and thermoplastic in addition to the wear analysis of the thermosetting composite fabricated. In future, thermoplastic matrixes can be reinforced with natural fibers using a twin screw extruder. Thermoplastic composites can replace metal composites and/or thermosetting composites in many applications. Currently a lot of research is going on in that area.

Once fabricated, mechanical, electrical, thermal as well as wear resistance attributes of thermoplastic composites reinforced with natural fibers can be compared with thermosetting composites reinforced with natural fibers as well as natural fiber reinforced metal matrix composites. This will help us replace the composites used currently with the best alternative in terms of properties desired as well as cost involved in component manufacturing.

REFERENCES

[1] R. Butola, A. Malhotra, M. Yadav, R. Singari, Q. Murtaza, P. Chandra, "Experimental Studies on Mechanical Properties of Metal Matrix Composites Reinforced with Natural Fibers Ashes," SAE Tech. P., 2019, https://doi.org/10.4271/2019-01-1123.

[2] OPEC, "The 13th edition of the World Oil Outlook (WOO) presents an in-depth review of the OPEC Secretariat's medium- to long-term projections and assessment for the global oil and energy industry," Panel Presentation at OPEC, Vienna, 2019.

[3] D. Toke, "The EU renewables directive—what is the fuss about trading?," Ener. Pol., vol. 36, no.8, pp.3001–3008, 2008.

[4] O. Faruk, A.K. Bledzki, H. Fink, M. Sain, "Biocomposites reinforced with natural fibers : 2000 – 2010," Prog. in Polym. Sci., vol. 37, no.11, pp.1552– 1596, 2012, doi:10.1016/j.progpolymsci.2012.04.003.

[5] D.N. Saheb, J.P. Jog, "Natural fiber polymer composites: A review," Adv. Poly. Tech., vol.18, no.4, pp.351–363, 1999, doi:10.1002/(SICI) 1098-2329(199924)18:4<>1.0.CO;2-Q.

[6] B.F. Yousif, N.S.M. El-Tayeb, "High-stress three body abrasive wear of treated and untreated oil palm fiber-reinforced polyester composite," J. Eng. Trib., vol.227, pp.385–392, 2013.

[7] G. Raju, C.T. Ratnam, N.A. Ibrahim, M.Z.A. Rahman, W. Yunus, "Enhancement of PVC/ENR blend properties by poly(methyl acrylate) grafted oil palm empty fruit bunch fiber," J. Appl. Polym. Sci., vol.110, pp.368–375, 2008, doi:10.1002/app.v110:1.

[8] S.V. Joshi, L.T. Drzal, A.K. Mohanty, S. Arora, "Are natural fiber composites environmentally superior to glass fiber reinforced composites?," Compos. A, vol.35, pp.371– 376, 2004.

[9] P. Wambua, J. Ivens, I. Verpoest, "Natural fibers: can they replace glass in fiber reinforced plastics?," Compos. Sci. Technol., vol.63, no.9, pp.1259–1264, 2003,https://doi.org/10.1016/s0266 &%23x00 AD;3538(03)00096 &%23x00 AD;4.

[10] C. Anubhav, N. Yuvaraj, R. Butola, T. Lakshay, "An experimental analysis of tensile, hardness and wear properties of aluminium metal matrix composite through

stir casting process," SN Appl. Sci., vol.2, p.892, 2020, https://doi.org/10.1007/s42452-020-2657-8.

[11] K.D. Sears, "Reinforcement of engineering thermoplastics with high purity cellulose fibers," *In Proc. sixth Int. conf. on wood fiber-plastic composites*, 2001, pp.27–34.

[12] T.H. Nam, S. Ogihara, N.H. Tung, S. Kobayashi, "Effect of alkali treatment on interfacial and mechanical properties of coir fiber reinforced poly (butylene succinate) biodegradable composites," Comp. Par. B: Eng., vol.42, no.6, pp.1648– 1656, 2011, doi:10.1016/j.compositesb.2011.04.001.

[13] S.J. Eichhorn, C.A. Baillie, N. Zafeiropoulos, L.Y. Mwaikambo, M.P. Ansell, A. Dufresne, P.M. Wild, "Review: Current international research into cellulosic fibers and composites," J. of Mat. Sci., vol.36, no.9, pp.2107–2131, 2001, doi:10.1023/A:1017512029696.

[14] T. Huber, J. Müssig, O. Curnow, S. Pang, S. Bickerton, M.P. Staiger, "A critical review of all-cellulose composites," J. Mat. Sci., vol.47, no.3, pp.1171– 1186, 2012, doi:10.1007/s10853-011-5774-3.

[15] X. Li, Æ.L.G. Tabil, Æ.S. Panigrahi, "Chemical treatments of natural fiber for use in natural fiber reinforced composites: A review," J. of Poly. & Env., pp.25–33, 2007, doi: 10.1007/s10924-006-0042-3.

[16] U.N., Food and Agriculture Organization of the United Nations FAO statistical yearbook. FAO, Rome, 2013.

[17] S. Sreenivasulu, A.C. Reddy, "Mechanical Properties Evaluation of Bamboo Fiber Reinforced Composite Materials," Int. J. of Eng. Res. (IJER), vol.3, no.1, pp.187-194, 2014.

[18] J.A. Olaitan, A.E. Terhemen, G.D. King, O.R. Oluwatoyin, "Comparative Assessment of Mechanical Properties of Groundnut Shell and Rice Husk Reinforced Epoxy Composites," Amer. J. of Mech. Eng., vol.5, no.3, pp.76-86, 2017, DOI:10.12691/ajme-5-3-2.

[19] S. Tamba, I. Cisse, F. Rendell, R. Jauberthie, "Rice husk in lightweight mortars," *In 2nd int. sym. on structural lightweight aggregate concrete*, 2000, pp.117–124.

[20] P. Mishra, A. Chakraverty, H.D. Banerjee, "Studies on physical and thermal properties of rice husk related to its industrial application," J. Mater. Sci., vol.21,

pp.2129– 2132, 1986.

[21] A. Kaupp, J.R. Goss, “Technical and economical problems in the gasification of rice hulls,” Phys. Chem. Prop. Energy Agric., vol.1, pp.201–234, 1982.

[22] S. Snehal, P. Lohani, “Silica nanoparticles: its green synthesis and importance in agriculture,” J. Pharmacogn. Phytochem., vol.7, no.5, pp.3383–3393, 2018.

[23] N. Thuadaij, A. Nuntiya, “Preparation of nanosilica powder from rice husk ash by precipitation method,” Chiang Mai J. Sci., vol.35, no.1, pp.206–211, 2008.

[24] A. Mahmud, M. Yusoff, F. Ahmad, “Processing of rice husk Tobio-silica nanoparticles through thermal combustion,” ARPN J. Eng. Appl. Sci., vol.11, no.12, pp.7650– 7654, 2016.

[25] S. Sankar, S.K. Sharma, D.Y. Kim, “Synthesis and characterization of mesoporous SiO2 nanoparticles synthesized from Biogenic Rice Husk Ash for optoelectronic applications,” Int. J. Eng. Sci., vol.17, pp.353–358, 2016.

[26] H. Chen, “Biogenic Silica Nanoparticles Derived from Rice Husk Biomass and Their Applications”, Ph.D. dissertation, Tex. St. Uni., Tex., USA, 2013.

[27] W.A.P.J. Premaratne, W.M.G.I. Priyadarshana, S.H.P. Gunawardena, A.A.P. De alwis, “Synthesis of nanosilica from paddy husk ash and their surface functionalization,” J. Sci. Univ. Kelaniya, vol.8, pp.33–48, 2013.

[28] I.D. Terkula, R.A. Wuana, M.S. Iorungwa, “Preparation and characterization of ‘green’ nano silica from rice husks,” Chem. Mater. Res., vol.9, no.6, pp.1–9, 2017.

[29] P.H. Dao, T.V. Nguyen, M.H. Dang, T.L. Nguyen, V.T. Trinh, M.V. Phuc, A.H. Nguyen, M.T. Duong, “Effect of silica nanoparticles on properties of coatings based on acrylic emulsion resin,” Vietnam J. Sci. Technol., vol.56, no.3B, pp.117–125, 2018.

[30] T. Kapur, T.C. Kandpal, H.P. Garg, “Electricity generation from rice husk in Indian rice mills: pottential and financial viability,” Biomass Bioenerg., vol.10, no.5–6, pp.393– 403, 1996.

[31] D. Chandramohan, L. Ravikumar, C. Sivakandhan, G. Murali, A. Senthilathiban, “Review on Tribological Performance of Natural Fiber-Reinforced Polymer Composites,” J. of Bio- and Tribo-Corr., vol.4, no.55, 2018, https://doi.org/10.1007/s40735-018-0172-x.

[32] A.L. Naidu, B. Sudarshan, K.H. Krishna, “Study On Mechanical Behavior Of Groundnut Shell Fiber Reinforced Polymer Metal Matrix Composites,” Int. J. of Eng.

Res. & Tech. (IJERT), vol.2, no.2, pp.2278-0181, 2013.

[33] G.C. Onuegbu, S.C. Nwanonenyi, M.U. Obidiegwu, "The effect of pulverised ground nut husk on some mechanical properties of polypropylene composites," Int. J. of Eng. Sc. Inv., vol.2, no.6, pp.79–83, 2013.

[34] M.A. Usman, I. Momohjimoh, A.I.S.B. Gimba, "Effect of groundnut shell powder on the mechanical properties of recycled polyethylene and its biodegradability," J. Miner Mater. Charact. Eng., vol.4, pp.228–240, 2016.

[35] G.U. Raju, S. Kumarappa, V.N. Gaitonde, "Mechanical and physical characterization of agricultural waste reinforced polymer composites," J. of Mat. Env. Sc., vol.3, pp.907-916, 2012.

[36] B.R. George, A. Bockarie, N. Bieak, A. Evazynajad, A. Kar, S. Veluswamy, H. McBride, "Textile products produced from alternative fibers," *In The Ninth Annual Conference on Recycling of Fibrous Textile and Carpet Waste*, Georgia, 2004.

[37] K. Raveendran, A. Ganesh, K.C. Khilart, "Influence of mineral matter on biomass pyrolysis characteristics," J. of Fuel, vol.74, p.1812, 1995.

[38] G.U. Raju, S.J. Kumarappa, "Experimental study on mechanical properties of groundnut shell particle reinforced epoxy composites," Reinf. Plast. Comp., vol.30, p.1029, 2011.

[39] H. Pihtili, "An experimental investigation of wear of glass fiber-epoxy resin and glass fiber- polyester resin composite materials," Eur. Poly. J., vol.45, pp.149–154, 2009, doi:10.1016/j.eurpolymj.2008.10.006.

[40] U. Nirmal, K.O. Low, J. Hashim, "On the effect of abrasiveness to process equipment using betelnut and glass fibers reinforced polyester composites," Wear, vol.290–291, pp.32–40, 2012.

[41] F.P. Mantia, M. Morreale, "Green composites: a brief review," Compos. A, vol.42, pp.579–588, 2011.

[42] Chawla, K. Krishnan, Composite materials. Science and engineering (3rd ed.), Springer-Verlag-New York, 2012.

[43] R. Butola, C. Pratap, A. Shukla, R. Walia, "Effect on the mechanical properties of aluminum-based hybrid metal matrix composite using stir casting method," Mater. Sci. Forum, vol.969, pp.253–259, 2019, https://doi.org/10.4028/www.scientifc.net/msf.969.253.

[44] A. Chaudhary, D.A. Kumar, A. Goel, R. Butola, M.S. Ranganath, “The Mechanical properties of different alloys in friction stir processing: a review,” Mater. Today, vol.5, no.2, pp.5553–5562, 2018, https://doi.org/10.1016/j.matpr.2017.12.146.

[45] Y. Mukesh, D. Kumar, R. Butola, M.S. Ranganath, “Effect of the impact strength of glass fiber reinforced plastic composite using wet layup process,” *In Mat. Today: Proc.*, 2020 https://doi.org/10.1016/j.matpr.2020.03.077.

[46] A. Shalwan, B.F. Yousif, “In state of art mechanical and tribological behaviour of polymeric composites based on natural fibers,” Mater. Des., vol.48, pp.14–24, 2013.

[47] M. Allen, M. Babiker, Y. Chen, H. de Coninck, S. Connors, R. van Diemen, O. Pauline Dube, K.L. Ebi, F. Engelbrecht, M. Ferrat, J. Ford, P. Forster, S. Fuss, T.G. Bolaños, J. Harold, O. Hoegh-Guldberg, J.C. Hourcade, D. Huppmann, D. Jacob, K. Jiang, T.G. Johansen, M. Kainuma, K. de Kleijne, E. Kriegler, D. Ley, D. Liverman, N. Mahowald, V. Masson-Delmotte, J.B. Robin Matthews, R. Millar, K. Mintenbeck, A. Morelli, W. Moufouma-Okia, L. Mundaca, M. Nicolai, C. Okereke, M. Pathak, A. Payne, R. Pidcock, A. Pirani, E. Poloczanska, H.O. Pörtner, A. Revi, K. Riahi, D.C. Roberts, J. Rogelj, J. Roy, S.I. Seneviratne, P.R. Shukla, J. Skea, R. Slade, D. Shindell, C. Singh, W. Solecki, L. Steg, M. Taylor, P. Tschakert, H. Waisman, R. Warren, P. Zhai, K. Zickfeld, “Summary for Policymakers,” UN IPCC, 2018.

[48] L. Dongdong, L. Bin, B. Chenguang, M. Minghui, X. Yan, Y. Chunyan, “Marine oil spill risk mapping for accidental pollution and its application in a coastal city,” Mar. Pollut. Bull, vol.96, no.1–2, pp.220–225, 2015.

[49] A.P.D.E. Souza et al, “Elevated CO2 increases photosynthesis, biomass and productivity, and modifies gene expression in sugarcane,” Pl. Cell Environ., vol.31, pp.1116–1127, 2008.

[50] J.R. Dufl, Y. Deng, K. Van Acker, W. Dewulf, “Do fiber reinforced polymer composites provide environmentally benign alternatives? A life-cycle-assessment-based study,” MRS Bull, vol.37, pp.374–382, 2012.

[51] V. Upadhyay, P.K. Jain, N.K. Mehta, “In-process estimate of roughness in turning of Ti–6Al–4V alloy using cutting constraints and vibration signals,” Meas., vol.46, pp.154–160, 2013.

[52] O. Tugrul, Y. Karpat, “Extrapolative modeling of roughness and tool wear in hard turning using regression and neural networks,” Int. J. of Mac. Tools & Manuf., vol.45, pp.467–479, 2005.

[53] R. Butola, Q. Murtaza, R.S. Walia, “Two start and Three Start Helical Abrasive Flow Machining for Brittle Materials,” *In Mat. Tod. Proc.*, 2017, vol.4, pp.3685-3693, https://doi.org/10.1016/j.matpr.2017.02.263.

[54] R. Butola, R. Jain, P. Bhangadia, A. Bandhu, R.S. Walia, Q. Murtaza, “Optimization to the parameters of abrasive flow machining by Taguchi method,” *In Mat. Today Proc.*, 2017, vol.5, 4720–4729.https://doi.org/10.1016/j.matpr.2017.12.044.

[55] R. Butola, M.S. Ranganath, Q. Murtaza, “Fabrication and optimization of AA7075 matrix surface composites using Taguchi technique via friction stir processing (FSP),” Eng. Res.Express, 2019, https://doi.org/10.1088/2631-8695/ab4b005.

[56] M.S. Ranganath, Vipin, R.S. Mishra, “Optimization of Process Parameters in Turning Operation of Aluminium (6061) with Cemented Carbide Inserts Using Taguchi Method and ANOVA,” Int. J. of Adv. Res. and Innov., vol.1, no.1, pp.13-21, 2013.

[57] M. Nalbant, H. Gokkaya, G. Sur, “Presentation of Taguchi method in the optimization of cutting parameters for roughness in turning,” Mat. and Des., vol.28, pp.1379–1385, 2007.

[58] P. Arbizu, C.J.L. Pérez, “Roughness estimate by factorial design of investigates in turning processes,” J. of Mat. Proc. Tech., vol.143– 144, pp.390–396, 2003.

[59] P.G. Benardos, G.C. Vosniakos, “Expecting roughness in machining: a review,” Int. J. of Mach. Tools & Manuf., vol.43, pp.833–844, 2003.

[60] M.S. Ranganath , Vipin, R.S. Mishra , Prateek, “Optimization of surface roughness in CNC turning of Aluminium 6061 using Taguchi Techniques,” Int. J. of Mod. Eng. Res. (IJMER), vol.5, pp.1-9, 2015.

[61] J. Schon, “Coefficient of friction of composite delamination surfaces,” Wear, vol.37, pp.77–89, 2000.

[62] P.D. Herrington, M. Sabbaghian, “Factors affecting the friction coefficients between metallic washers and composite surfaces,” Comp., vol.22, pp.418–424, 1991.

[63] X.H. Zhou, Y.S. Sun, W.S. Wang, “Influences of carbon fabric/epoxy composites fabrication process on its friction and wear properties,” J. of Mat. Proc. Tech., vol.209, pp.4553–4557, 2009.

[64] P. Jost, “Tribology: how a word was coined 40 years ago,” Tribol. Lubr. Technol., vol.62, p.24, 2006.

[65] S. Abarou, D. Play, “Wear transition of self-lubricating composites used in dry oscillating applications,” ASLE Trans., vol.30, no.3, p p . 269–281, 1986.

[66] P. Rehbein, J. Wallaschek, “Friction and wear behavior of polymer/steel and alumina/alumina under high frequency fretting conditions,” Wear, vol.216, pp.97–105, 1998.

[67] S. Karthikeyan, N. Rajini, S. Jacob, T. Winowlin, D.B. Patrick, “Dry sliding wear properties of Jute/polymer composites in high loading applications,” Trans-Trio Sci., vol.12, pp.7-18, 2015.

[68] O. Faruk, A.K. Bledzki, H.P. Fink, M. Sain, “Biocomposites reinforced with natural fibers,” Prog. Polym. Sci., vol.37, no.11, pp.1552–96, 2012.

[69] R. Vinayagamoorthy, “Friction and wear characteristics of fiber reinforced plastic composites,” J. of Thermoplas. Comp. Mat., pp.1–23, 2018, DOI: 10.1177/0892705718815529.

[70] A. Pogosian, K. Hovhannisyan, A. Isajanyan, “Polymer Friction Transfer (FT),” In: WangQJ, ChungY-W, editors. Encyclopedia of Tribology, SE-820. SpringerUS, 2585–92, 2013.

[71] A.K. Pogosian, “Forecasting the viability of friction pairs in accelerated tests,” Wear, vol.26, pp.175–86, 1973.

[72] K. Kato, “Classification of wear mechanisms/models,” Proc. IMechE. J. Eng. Tribol., vol.216, pp.349–355. 2002.

[73] T. Sunil , S. Chauhan , “Effect of micron and submicron size cenosphere particulate on mechanical and tribological characteristics of vinylester composites,” Proc. IMechE J. Eng. Tribol.,vol.228, pp.415–423, 2014.

[74] Q. Lehua, G. Pan, Y. Fu, et al., “Effect of MoS2 on the tribological properties of carbon fabric composites under wet conditions,” Proc. IMechE J. Eng. Tribol., vol.232, pp.126–135, 2018.

[75] Z. Shaofeng, Q. Zhang, J. Huang, et al., “Friction and wear behaviors of polyamide- based composites blended with polyphenylene sulfide,” J. Thermoplast. Compos. Mater., vol.27, pp.977–991, Huang.

[76] C. Haizheng, X. Cheng, “Mechanical and tribological properties of MWCNTs-

reinforced thermoplastic poly(p-oxybenzoate) composites," J. Reinf. Plast. Compos., vol.31, pp.785–795, 2012.

[77] S.P. Samantrai, G. Raghavendra, S.K. Acharya, "Effect of carbonization temperature and fiber content on the abrasive wear of rice husk char reinforced epoxy composite," Proc. IMechE J. Eng. Tribol., vol.228, pp.463–469.

[78] H. Imrek, S.M. Demet, "Experimental investigation of wear behaviors of bronze and carbonreinforced polytetrafluoroethylene alloy pivot pin bearings," Proc. IMechE J. Eng. Tribol., vol.228, pp.1187–1194, 2014.

[79] M.S. Ranganath, Vipin , R.S. Mishra , P. Jain, S. Kumar, "Experiment Investigation of surface roughness and cutting force on conventional dry turning of aluminium (6061)," Int. J. of Mod. Eng. Res. (IJMER), vol.5, pp.14-23, 2015.

[80] A. Hamdi, A.Y. Mohamed, K. Chaoui, T. Mabrouki, J.F. Rigal, "Exploration of roughness and cutting force elements in hard turning with CBN tool: Prediction model and cutting conditions optimization," Measur.,vol.45, pp.344–353, 2012.

[81] J. Davim, V.N. Gaitonde, S.R. Karnik, "Inquiries into the effect of cutting circumstances on roughness in turning of free machining steel by ANN models," J. of mat. Administ. Tech., vol.205, pp.16–23, 2008.

[82] I.A. Choudhury, M.A. EI-Baradie, "Roughness estimate in the turning of high-strength steel by factorial design of tests," J. of Mat. Proc. Tech., vol.67, pp.55-61, 1997.

[83] W.H. Yang, Y.S. Tarng, "Strategy optimization of cutting constraints for turning operations based on the Taguchi method," J. of Mat. Proc. Tech., vol.84, pp.122–129.

[84] I. Asilturk, H. Akkus, "Determining the effect of cutting constraint on roughness in hard turning using the Taguchi method," Measur., vol.44, pp.1697–1704, 2011.

[85] D. Freedman, Statistical Models: Theory and Practice. 2nd edn. Cambridge University Press, Cambridge, 2009.

[86] Y. Xin, Linear Regression Analysis: Theory and Computing. 1st edn. World Scientific, Singapore, 2009.

[87] D. Montgomery, E. Peck, G. Vining , Introduction to Linear Regression Analysis. 5th edn. Wiley Publishers, USA, 2012.

[88] N.S. Altman, "An introduction to kernel and nearest-neighbor nonparametric regression," T. Amer. Stat., vol.46, no.3, pp.175–185.

[89] C. Corinna, N.V. Vladimir, “Support-vector networks,” Mach. Lear., vol.20, no.3, p p . 273–297, 1995.

[90] V.N. Vapnik, The nature of statistical learning theory. 2nd edn. Springer, New York, 2000.

[91] A. Smola, B. Schölkopf, “A tutorial on support vector regression,” Stat. & Comp., vol.14, pp.199–222, 2004.

[92] L. Pasanen, L. Holmström, M.J. Sillanpää, “Supporting Information for Bayesian LASSO, scale space and decision making in association genetics,” PLoS ONE, vol.10, pp.4, 2015.

[93] M.E. Tipping, “Sparse Bayesian Learning and the Relevance Vector Machine,” J. of Mach. Lear. Res., vol.1, 2001.

[94] D.J.C. MacKay , “Bayesian Interpolation,” Comp. & Neu. Sys., vol.4, no.3, 1992.

[95] J.R. Quinlan, “Induction of Decision Trees,” Mach. Lear., vol.1, pp.81-106, 1986.

[96] L. Brelman, “Arcing the Edge,” Tech. Rep. 486, Statistics Department University of California, Berkeley, USA, 1997.

[97] J.J. Hopfield, “Neural networks and physical systems with emergent collective computational abilities,” Proc. Natl. Acad. Sci. U S A, vol.79, no.8, p p . 2554–2558, 1982.

[98] D.E. Goldberg, Genetic Algorithms in Search Optimization and Machine Learning. 1st edn. Addison-Wesley Publishing Company Inc., Reading MA, 1989.

[99] D.L. Carroll, “Chemical Laser Modeling with Genetic Algorithms,” AIAA J., vol.34, no.2, pp.338–346, 1996.

[100] G. Winter, P. Cuesta, J. Periaux, M. Galan, P. Cuesta, Genetic algorithm in engineering and computer science, Wiley, New York, 1996.

[101] E. Bagci, B. Işık, “Examination of roughness in turning unidirectional GFRP syntheses by using RS approach and ANN,” Int. J. Adv. Manuf. Technol., vol.31, pp.10–17, 2006.

[102] B.Y. Lee, Y.S. Tarng, “Roughness assessment by computer visualization in turning processes,” Int. J. of Mach. Tools & Manuf., vol.41, pp.1251– 1263, 2001.

[103] G.U. Raju, S. Kumarappa, “Experimental study on mechanical properties of groundnut shell particle reinforced epoxy composites,” J. of Reinf. Plas. & Comp., vol.30, no.12, pp.1029–1037, 2016, DOI: 10.1177/0731684411410761.

[104] M. Belin, “Triboscopy: a new quantitative tool for microtribology,” Wear, vol.168, pp.7–12, 1993.

[105] A. Ruggiero, M. Merola, P. Carlone, V.M. Archodoulaki, “Tribo-mechanical characterization of reinforced epoxy resin under dry and lubricated contact conditions,” Comp. P. B, vol.79, pp.595-603, 2015.

Appendix

```
#For Surface Roughness
from sklearn.metrics import mean_squared_error
from sklearn.model_selection import train_test_split
#from sklearn import preprocessing
X=[[1.67, 0, 0],[1.67, 0.04, 0.04],[1.67, 0.08, 0.08],[2, 0, 0.04],[2, 0.04, 0.08],[2, 0.08,
    0],[3, 0, 0.08],[3, 0.04, 0],[3, 0.08, 0.04]]
y=[1.97,2.27,2.96,1.87,2.14,2.02,1.94,1.66,2.17]
X_train, X_test, y_train, y_test = train_test_split(X, y, test_size=0.33, random_state=42)
"""
ytr_scaled = abs(preprocessing.scale(y_train))
yte_scaled = abs(preprocessing.scale(y_test))
y_scaled = abs(preprocessing.scale(y))
print(abs(y_scaled))
"""
#Linear Regression
from sklearn import linear_model
clf=linear_model.LinearRegression()

clf.fit(X_train, y_train)
pred12=clf.predict(X_test)
print(abs(pred12))
print('Accuracy is: {}'.format(mean_squared_error(y_test,pred12)))

print("Function for Linear Regression")
m = clf.coef_
b = clf.intercept_
print(' y = {0} * x + {1}'.format(m, b))
```

```
#KNN regression
from sklearn.neighbors import KNeighborsRegressor
neigh = KNeighborsRegressor(n_neighbors=2)


 #for SR
neigh.fit(X_train, y_train)
pred22=neigh.predict(X_test)
print(abs(pred22))
print('Accuracy is: {}'.format(mean_squared_error(y_test,pred22)))

#SVR
from sklearn.svm import SVR
regressor=SVR(kernel='linear')

  #for SR
regressor.fit(X_train, y_train)
pred32=regressor.predict(X_test)
print(abs(pred32))
print('Accuracy is: {}'.format(mean_squared_error(y_test,pred32)))

print("Function for SVR")
m = regressor.coef_
b = regressor.intercept_
print(' y = {0} * x + {1}'.format(m, b))
```

```
#Bayesian Ridge
model=linear_model.BayesianRidge()

 #for SR
model.fit(X_train, y_train)
pred42=model.predict(X_test)
print(abs(pred42))
print('Accuracy is: {}'.format(mean_squared_error(y_test,pred42)))

print("Function for Bayesian Ridge")
m = model.coef_
b = model.intercept_
print(' y = {0} * x + {1}'.format(m, b))

#Decision Tree Regression
from sklearn import tree
dtr = tree.DecisionTreeRegressor()

  #for SR
dtr.fit(X_train, y_train)
pred52=dtr.predict(X_test)
print(abs(pred52))
print('Accuracy is: {}'.format(mean_squared_error(y_test,pred52)))

#GradientBoostingRegressor
from sklearn.ensemble import GradientBoostingRegressor
gbr =GradientBoostingRegressor()
```

```
 #for SR
gbr.fit(X_train, y_train)
pred62=gbr.predict(X_test)
print(abs(pred62))
print('Accuracy is: {}'.format(mean_squared_error(y_test,pred62)))
#SR_true vs SR_pred
xdp=[1,2,3]
import matplotlib.pyplot as plt
plt.plot(xdp,y_test,'rs')
plt.plot(xdp,pred12,'b--',label='linear regression')
plt.plot(xdp,pred22,'g--',label='KNN')
plt.plot(xdp,pred32,'c--',label='SVR')
plt.plot(xdp,pred42,'m--',label='Bayesian Ridge')
plt.plot(xdp,pred52,'y--',label='Decision Tree')
plt.plot(xdp,pred62,'k--',label='Gradient Boosting Regression')
#plt.plot(xdp,pred72,'r--',label='Neural Network')
plt.title('Regression for SR_true vs SR_pred')
plt.xlabel('No. of datapoints')
plt.ylabel('SR')
plt.legend(loc='upper right',bbox_to_anchor=(1.6,1))
plt.show()
```

Table: Wear analysis data for sample L1

TIME	COF	FF	TEMP	LOAD
0.151	-0.001	-0.012	16.863	9
59.991	0.146	1.31	17.631	9
120.051	0.158	1.423	17.75	9
180.028	0.176	1.582	18.061	9
240.1	0.196	1.765	18.595	9
300.033	0.221	1.99	18.681	9
360.027	0.248	2.233	18.579	9
420.064	0.288	2.594	18.811	9
480.005	0.356	3.2	18.671	9
540.104	0.488	4.391	19.131	9
600.01	0.593	5.335	19.317	9
660.054	0.679	6.112	18.734	9
720.035	0.703	6.325	18.83	9
780.07	0.738	6.639	19.313	9
840.094	0.75	6.749	19.181	9
900.029	0.763	6.87	19.747	9
960.091	0.781	7.031	19.28	9
1020.026	0.797	7.172	19.559	9
1080.075	0.804	7.233	19.425	9
1140.029	0.818	7.362	19.443	9
1200.049	0.825	7.423	19.5	9
1260.016	0.807	7.259	19.863	9
1320.136	0.827	7.44	19.535	9
1380.012	0.875	7.874	19.523	9
1440.05	0.881	7.929	19.434	9
1500.144	0.899	8.091	19.606	9
1560.003	0.916	8.242	19.059	9
1620.034	0.92	8.277	19.572	9
1680.088	0.927	8.347	19.706	9
1740.085	0.939	8.45	20.04	9
1800.053	0.937	8.435	19.624	9
1860.013	0.943	8.491	19.686	9
1920.002	0.943	8.491	20.124	9
1980.004	0.94	8.461	19.882	9
2040.062	0.949	8.538	19.611	9
2100.07	0.951	8.563	20.309	9
2160.077	0.953	8.58	19.972	9
2220.011	0.96	8.639	19.868	9
2280.026	0.964	8.68	19.718	9
2340.021	0.961	8.645	19.967	9
2399.926	0.953	8.58	19.99	9

Table: Wear analysis data for sample L3

TIME	COF	FF	TEMP	LOAD
0.149	0.002	0.016	18.005	9
60.13	0.189	1.705	18.629	9
120.013	0.201	1.807	18.992	9
180.128	0.208	1.876	19.304	9
240.091	0.213	1.918	19.664	9
300.116	0.215	1.938	19.782	9
360.083	0.216	1.947	20.058	9
420.025	0.22	1.976	20.157	9
480.054	0.221	1.987	20.278	9
540.068	0.222	2	20.372	9
600.009	0.223	2.006	20.541	9
660.114	0.224	2.013	20.499	9
720.12	0.224	2.02	20.565	9
780.019	0.225	2.028	20.655	9
840.043	0.226	2.033	20.535	9
900.057	0.228	2.052	20.844	9
960.007	0.229	2.065	20.844	9
1020.105	0.23	2.074	20.864	9
1080.001	0.231	2.081	20.9	9
1140.022	0.233	2.097	20.95	9
1200.069	0.234	2.109	20.919	9
1260.074	0.235	2.119	21.088	9
1320.04	0.236	2.128	20.926	9
1380.07	0.239	2.154	21.056	9
1440.105	0.239	2.155	21.178	9
1500.035	0.24	2.164	21.043	9
1560.062	0.24	2.164	21.122	9
1620	0.242	2.175	21.074	9
1680.033	0.24	2.16	21.076	9
1740.014	0.242	2.18	21.142	9
1800.054	0.243	2.183	21.167	9
1860.099	0.243	2.186	21.18	9
1920.129	0.245	2.202	21.075	9
1980.068	0.245	2.208	21.368	9
2040.043	0.247	2.226	21.241	9
2100.008	0.247	2.227	21.169	9
2160.083	0.248	2.234	21.358	9
2220.074	0.249	2.243	21.049	9
2280.066	0.251	2.258	21.21	9
2340.086	0.251	2.261	21.345	9
2399.967	0.252	2.264	21.2	9

Table: Wear analysis data for sample L4

TIME	COF	FF	TEMP	LOAD
0.149	-0.011	-0.101	20.548	9
60.061	0.308	2.774	20.389	9
120.056	0.312	2.807	21.178	9
180.113	0.319	2.869	20.854	9
240.051	0.324	2.916	21.465	9
300.005	0.33	2.97	21.667	9
360.081	0.331	2.982	20.997	9
420.064	0.341	3.067	21.844	9
480.035	0.344	3.097	21.783	9
540.018	0.35	3.151	22.531	9
600.062	0.353	3.175	21.487	9
660.072	0.358	3.221	21.891	9
720.066	0.36	3.242	21.991	9
780.139	0.364	3.272	21.993	9
840.013	0.369	3.318	21.941	9
900.087	0.367	3.301	22.356	9
960.034	0.374	3.369	22.514	9
1020.029	0.376	3.383	22.591	9
1080.079	0.379	3.411	22.488	9
1140.074	0.381	3.433	21.534	9
1200.039	0.381	3.433	22.482	9
1260.136	0.383	3.447	22.217	9
1320.013	0.381	3.426	22.225	9
1380.004	0.382	3.434	22.741	9
1440.07	0.391	3.519	22.756	9
1500.013	0.392	3.53	22.256	9
1560.077	0.392	3.532	22.232	9
1620.01	0.397	3.576	22.444	9
1680.009	0.402	3.62	22.972	9
1740.008	0.402	3.621	22.455	9
1800.094	0.404	3.636	22.538	9
1860.074	0.402	3.618	22.841	9
1920.05	0.404	3.639	22.656	9
1980.013	0.406	3.658	22.297	9
2040.04	0.41	3.693	22.531	9
2100.03	0.407	3.662	22.535	9
2160.225	0.41	3.694	23.011	9
2220.001	0.411	3.697	22.844	9
2280.009	0.412	3.712	22.633	9
2340.045	0.415	3.734	23.116	9
2399.938	0.415	3.738	22.541	9

Table: Wear analysis data for sample L6

TIME	COF	FF	TEMP	LOAD
0.198	-0.009	-0.082	19.625	9
60.057	0.327	2.945	19.332	9
120.046	0.37	3.329	20.262	9
180.083	0.391	3.519	20.314	9
240.1	0.406	3.651	20.272	9
300.056	0.425	3.821	20.93	9
360.097	0.435	3.918	21.015	9
420.047	0.445	4.002	21.329	9
480.149	0.451	4.063	20.974	9
540.04	0.462	4.157	21.388	9
600.026	0.475	4.278	21.512	9
660.021	0.482	4.341	21.132	9
720.067	0.489	4.397	21.608	9
780.011	0.494	4.446	21.116	9
840.012	0.487	4.381	21.622	9
900.087	0.493	4.436	21.743	9
960.131	0.514	4.626	21.608	9
1020.026	0.505	4.542	21.873	9
1080.073	0.502	4.515	22.2	9
1140.073	0.525	4.725	21.961	9
1200.066	0.534	4.804	21.841	9
1260.069	0.528	4.754	21.813	9
1320.026	0.537	4.833	22.043	9
1380.075	0.541	4.87	21.941	9
1440.122	0.551	4.959	21.98	9
1500.079	0.552	4.966	21.84	9
1560.043	0.555	4.998	21.97	9
1620.07	0.556	5.004	22.116	9
1680.108	0.556	5.006	21.944	9
1740.007	0.542	4.878	21.951	9
1800.052	0.55	4.95	22.682	9
1860.013	0.555	4.992	22.082	9
1920.074	0.573	5.158	21.996	9
1980.024	0.577	5.194	22.281	9
2040.06	0.583	5.251	22.607	9
2100.104	0.578	5.203	21.661	9
2160.06	0.579	5.208	22.274	9
2220.026	0.562	5.058	22.151	9
2280.03	0.58	5.22	22.366	9
2340.008	0.588	5.291	22.85	9
2399.87	0.588	5.293	23.119	9

Springer

ICAPIE

Date: 25/05/2020

Certificate of Acceptance

Dear Author(s): Susheem Kanwar, Vipin, Ranganath M. Singari

Paper ID: 012

Paper Title: Prediction of Material Removal Rate and Surface Roughness in CNC Turning of Delrin using various Regression techniques and Neural Networks and Optimization of Parameters using Genetic Algorithm

This is to enlighten you that above manuscript appraised by the proficient and it is accepted by the editors of **Advances in Manufacturing and Industrial Engineering: Select Proceedings of ICAPIE 2019** for publication in the book series **Lecture Notes in Mechanical Engineering (Scopus Indexed)** ISSN: 2195-4356. The manuscript was submitted in April 2020 and will be online during September 2020.

Finally, the team of LNME and ICAPIE would like to further extend congratulations to you.

Editor- Conference Proceeding

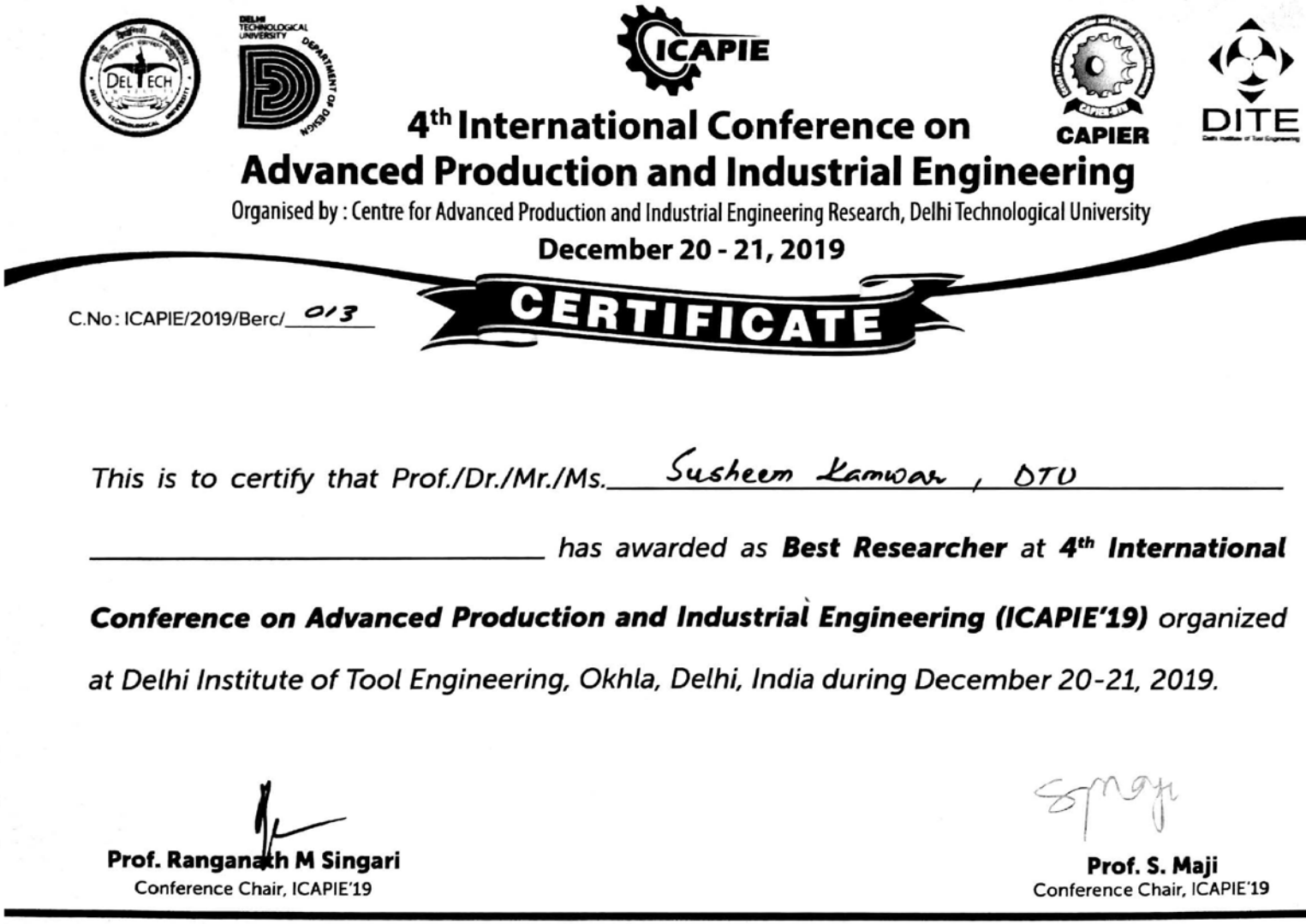

4th International Conference on Advanced Production and Industrial Engineering

Organised by : Centre for Advanced Production and Industrial Engineering Research, Delhi Technological University

December 20 - 21, 2019

C.No : ICAPIE/2019/Berc/013

CERTIFICATE

This is to certify that Prof./Dr./Mr./Ms. Susheem Kamwar, DTU

_____ *has awarded as* ***Best Researcher*** *at* ***4th International Conference on Advanced Production and Industrial Engineering (ICAPIE'19)*** *organized at Delhi Institute of Tool Engineering, Okhla, Delhi, India during December 20-21, 2019.*

Prof. Ranganath M Singari
Conference Chair, ICAPIE'19

Prof. S. Maji
Conference Chair, ICAPIE'19

Gmail susheem kanwar <sushkanwar@gmail.com>

Fwd: Your Submission JMM-2020-0031R1 is Accepted

1 message

Ravi Butola <ravibutola33855@gmail.com> Wed, Jul 1, 2020 at 2:46 PM
To: susheem kanwar <sushkanwar@gmail.com>

---------- Forwarded message ---------
From: **Journal Office** <em@editorialmanager.com>
Date: Mon 29 Jun, 2020, 11:06 PM
Subject: Your Submission JMM-2020-0031R1 is Accepted
To: RAVI BUTOLA <ravibutola33855@gmail.com>

SAE INTERNATIONAL

Ref.: SAE International Journal of Materials and Manufacturing
Manuscript Number: JMM-2020-0031R1
Comparison of Genetic Algorithm and Taguchi technique for surface roughness of natural fiber reinforced polymer composites

Dear Mr BUTOLA,

I am pleased to tell you that your work has now been accepted for publication in SAE International Journal of Materials and Manufacturing. It was accepted on 06/29/2020. If any, Comments from the Editor and Reviewers can be found below. Please note that your manuscript is accepted as-is, and no further revisions are required. You will be able to make any minor, necessary edits at the author proofing stage.

Please send a list of SAE International Customer Numbers/Member ID Numbers for all authors to managingeditor@sae.org. If any author does not know his or her customer number, or needs to create one, please visit my.sae.org and follow the instructions there. *Your article cannot move into the production process until this comprehensive list has been received.*

After the Customer Numbers/Member ID Numbers for all authors are received, your article will then enter the production process where your article will be put into the proper SAE format. You will receive an automated email notification that your article has been published, however this is referring to your author submitted manuscript only. Shortly after you sign off on your author proof of your SAE formatted manuscript, the formatted version will replace your author submitted manuscript with an e-first version, and the final paginated version will replace the e-first version when the issue is compiled.

Thank you for submitting your work to this journal.

With kind regards,
SAE International Journal of Materials and Manufacturing

NYU | TANDON SCHOOL OF ENGINEERING

Susheem Kanwar
Pocket E 597 Mayur Vihar Phase 2
Delhi, Delhi 110091
India

Degree: Doctorate in Mechanical Engineering
Term: Fall 2020
Method: In Person
NYU ID Number: [redacted]
Net ID: [redacted]

2020-02-07

Dear Susheem,

Congratulations! It is my distinct pleasure to offer you admission to the Doctorate in Mechanical Engineering program at NYU Tandon School of Engineering as a Full Time student.

As an NYU Tandon School of Engineering graduate student, you will discover the resources and inspiration to turn your research into innovations, products, services, and entrepreneurial ventures. You will also enjoy the benefits of:

- Our world-class faculty, engaged in cutting edge research at the boundaries between disciplines. Students and faculty share a passion for the creation and execution of world class research and projects with global impact.
- A rigorous graduate curriculum that will develop your technical knowledge and introduce you to latest developments in your area of specialty, preparing you for leadership positions throughout your career.
- A diverse environment for worldwide academic collaboration. New York University is a global university providing you with the opportunity to work with students and faculty from around the world.

This is an exciting time to be joining the NYU Tandon School of Engineering. You and your future classmates have demonstrated the academic accomplishments and leadership potential that will support your success in our graduate programs, which have been a hallmark of NYU School of Engineering for more than 110 years.

To accept the offer of admission and reserve a space in the Fall 2020 class before the deadline of May 1, 2020, visit your personalized dashboard at **gradadmit.engineering.nyu.edu**. There, you will also find information about your curriculum, ways to connect with fellow classmates, and information about upcoming admitted student events.

Susheem, I look forward to greeting you in the coming months. I have no doubt that you will make significant contributions to our community of scholars, researchers and professionals. Welcome to NYU Tandon School of Engineering.

Sincerely,

Elizabeth Ensweiler

Elizabeth Fern Ensweiler M.Ed
Senior Director, Graduate Enrollment Management and Admissions